

1 **Ammonium sensitivity of biological nitrogen fixation in anaerobic diazotrophs and**
2 **coastal salt marsh sediments.**

3
4 Romain Darnajoux¹, Linta Reji¹, Xin Rei Zhang^{1,2}, Katja E. Luxem¹, and Xinning Zhang^{1, 2}

5
6 ¹Department of Geosciences, Princeton University, Princeton, 08544, NJ, USA

7 ²High Meadows Environmental Institute, Princeton University, Princeton, 08544, NJ, USA

8
9 Corresponding author: RD and XZ

10 ORCID: RD: 0000-0002-4996-0067, XZ: 0000-0003-2763-1526, KEL: 0000-0001-7310-0668,

11 LR: 0000-0002-1337-6782

12
13 Key points:

- 14
- 15 • We identified a porewater ammonium concentration threshold of 9 μM for biological
16 nitrogen fixation inhibition in benthic environments.
 - 17 • Drawdown of porewater ammonium, timing of enzyme inhibition, and sediment
18 heterogeneity can complicate measurement of nitrogen sensitivity.
 - 19 • Review of porewater ammonium concentration indicates biological nitrogen fixation is
20 likely limited to the superficial layer of sediments.
- 21

22 **Abstract:**

23 New bioavailable nitrogen (N) from biological nitrogen fixation (BNF) is critical for the N
24 budget and productivity of marine ecosystems. Nitrogen-fixing organisms typically inactivate
25 BNF when less metabolically costly N sources, like ammonium (NH_4^+), are available. Yet,
26 several studies observed BNF in benthic marine sediments linked to anaerobic sulfate-
27 reducing bacteria (SRB) and fermenting firmicutes despite high porewater NH_4^+
28 concentrations (10-1,500 μM), making the importance of and regulating controls on benthic
29 BNF unclear. Here, we evaluate BNF sensitivity to NH_4^+ in model anaerobic diazotrophs, the
30 sulfate-reducer *Desulfovibrio vulgaris* var. Hildenborough and fermenter *Clostridium*
31 *pasteurianum* strain W5; in sulfate-reducing sediment enrichment cultures, and in sediment
32 slurry incubations from three Northeastern salt marshes (USA). BNF in sulfate-reducing
33 cultures and sediments is highly sensitive to external NH_4^+ , with a threshold for BNF
34 inhibition of $[\text{NH}_4^+] < 2 \mu\text{M}$ in cultures and $< 9 \mu\text{M}$ in sediment slurries. The prevalence of
35 SRB-like sequences in sediment-derived nitrogenase (*nifH*) genes and transcripts in this and
36 other studies of benthic BNF along with an analysis of benthic NH_4^+ porewater data suggests
37 a broad applicability of the inhibition thresholds measured here and the confinement of
38 benthic BNF to surficial sediments. The timing of inhibition, fast NH_4^+ drawdown, and
39 sediment heterogeneity are factors that can complicate studies of benthic BNF sensitivity to
40 NH_4^+ . We propose a simple theoretical framework based on the affinity of the NH_4^+
41 transporter to explain NH_4^+ control of BNF and improve biogeochemical models of N cycling.

42

43

44 Introduction

45 The requirement for bioavailable fixed nitrogen (N) is a fundamental constraint for all
46 life on Earth. Biological nitrogen fixation (BNF), the only biological process capable of
47 producing newly fixed N, is critical for the function and ecology of the biosphere. Present in a
48 small subset of taxonomically and metabolically diverse prokaryotes termed diazotrophs, all
49 BNF is catalyzed by the enzyme nitrogenase in a complex, energy-intensive reaction that
50 reduces dinitrogen (N_2) into ammonia (NH_3), which is subsequently incorporated into cell
51 material. Diazotrophs thus function as natural gatekeepers for ecosystem N input and are
52 particularly important in oligotrophic systems, such as the surface waters of the tropical and
53 subtropical ocean (Sohm et al., 2011; Voss et al., 2013; Zehr & Kudela, 2011), where low,
54 nanomolar levels of dissolved inorganic fixed N species (DIN *i.e.*, ammonium NH_4^+ , nitrite
55 NO_2^- , nitrate NO_3^-) limit primary production (Elser et al., 2007).

56 The distribution of BNF in marine waters was traditionally explained by the well-
57 documented regulation of nitrogenase synthesis and activity by DIN in model cyanobacterial
58 and aerobic diazotrophs (*e.g.*, *Trichodesmium* and *Azotobacter*), which downregulate BNF
59 when ambient DIN concentrations are sufficient to meet cell anabolic demands (*e.g.*,
60 external $[NH_4^+] >$ hundreds of nanomolar to tens of micromolar, depending on the species
61 (Drozd et al., 1972; Hartmann et al., 1986; Holl & Montoya, 2005; Kleiner, 1974; Mulholland
62 et al., 2001; Ohki et al., 1991; Postgate & Kent, 1984). This downregulation reflects the high
63 energetic cost of N acquisition through BNF, in comparison to the metabolic cost of
64 assimilating NH_4^+ or NO_3^- (Glibert et al., 2016; Großkopf & LaRoche, 2012; Inomura et al.,
65 2017). Accordingly, marine BNF in hypoxic and anoxic benthic environments, where
66 porewater NH_4^+ concentrations are typically orders of magnitude higher than in euphotic
67 zones (see Knapp and reference therein) (Knapp, 2012), has been estimated to account for
68 only 10% of total marine new N inputs, with benthic BNF largely restricted to highly
69 productive shallow sedimentary environments like seagrass meadows (Capone, 1988;
70 Capone & Carpenter, 1982; Zhang et al., 2020).

71 However, recent studies ranging from open ocean to coastal estuary benthic systems
72 have challenged the above paradigm based on observations of BNF activity and nitrogenase
73 (*nifH*, *nitrogenase reductase*) genes and transcripts in sediments with high porewater NH_4^+
74 concentrations (e.g. ~ 50-1500 μM) (Bertics et al., 2013; Gier et al., 2016; Knapp, 2012).
75 These results, many obtained with closed vessel sediment incubation experiments, have led
76 to the proposal that benthic BNF may be a larger contribution to marine N inputs than
77 previously thought (Fulweiler et al., 2007; Newell, McCarthy, et al., 2016; David T. Welsh,
78 2000). At a larger scale, increased benthic BNF has been suggested to help resolve an
79 apparent and highly debated imbalance in the modern marine N budget (Codispoti, 2007;
80 Gruber & Galloway, 2008; Zhang et al., 2020). A better understanding of the ecophysiology
81 of benthic diazotrophs, particularly how such microorganisms regulate BNF under fluctuating
82 environmental conditions, is necessary to resolve questions of when and why BNF occurs in
83 benthic settings and to ascertain its importance to the marine N cycle.

84 Molecular surveys of the nitrogenase gene *nifH* (Bertics et al., 2010; Kapili et al.,
85 2020; Newell, Pritchard, et al., 2016; Zehr et al., 2003) and activity assays designed to target
86 specific microbial groups (e.g., molybdate additions, sulfide production) (Bertics et al., 2010;
87 Gandy & Yoch, 1988; Newell, Pritchard, et al., 2016; D. T. Welsh et al., 1996) have identified
88 sulfate-reducing bacteria (SRB), such as *Desulfovibrio* sp., as the dominant N_2 fixers in
89 benthic systems (Brown & Jenkins, 2014; Dekas et al., 2018; Gier et al., 2015; Kapili et al.,
90 2020; Newell, McCarthy, et al., 2016). Fermentative firmicute species (e.g. *Clostridium* sp.)
91 have also been consistently observed in surveys of benthic diazotrophy (Gier et al., 2016;
92 Kapili et al., 2020). Such data, which imply a very low sensitivity of BNF to DIN in SRB and
93 Clostridia, have been used to suggest that the physiology and purpose of BNF in benthic
94 organisms could be fundamentally different from that of euphotic zone N_2 fixers (Knapp,
95 2012). For example, BNF at high NH_4^+ (e.g. $[\text{NH}_4^+] > 50 \mu\text{M}$) has been taken as a sign that
96 benthic microorganisms may be using BNF to balance intracellular redox under reducing
97 conditions (Tichi & Tabita, 2000). While this paradox has important implications for our

98 understanding of marine N cycling, the physiologies of N₂ fixation in SRB and other anaerobic
99 diazotrophs have garnered little attention compared to the aerobic and phototrophic
100 diazotrophs (Gordon et al., 1981; Postgate & Kent, 1984; Riederer-Henderson & Wilson,
101 1970; Tubb & Postgate, 1973).

102 Here, we examine N₂ fixation by the model SRB *Desulfovibrio vulgaris* var.
103 Hildenborough (*DvH*) (Heidelberg et al., 2004) and the model fermenter *Clostridium*
104 *pasteurianum* strain W5 (*Cp*) (Winogradsky, 1895), two free-living diazotrophic species
105 common in sediments (Brown & Jenkins, 2014), and in sulfate-reducing sediments from
106 three salt marshes along the Northeastern coast of the United States. By simultaneously
107 tracking BNF activity and ambient NH₄⁺ concentrations in liquid culture incubations, we find
108 that BNF by *DvH* only occurs once NH₄⁺ concentrations fall below ~ 2 μM and < 20 μM in *Cp*,
109 where we had lower data resolution. In sediment slurry incubations assayed using two
110 independent methods (acetylene reduction assay and ¹⁵N tracer), the NH₄⁺ threshold for
111 BNF inhibition is ~ 9 μM. The data indicate benthic BNF is more sensitive to fixed N than
112 recent studies would suggest and similar to the NH₄⁺ sensitivity of BNF by diverse cultured
113 diazotrophs. Analyses of nitrogen fixation genes and porewater NH₄⁺ data suggest the broad
114 relevance of the ammonium threshold measured. We find that the timing of BNF inhibition by
115 NH₄⁺, the fast removal of ambient NH₄⁺ by active microorganisms, and the heterogeneous
116 nature of sediments must be considered when investigating the NH₄⁺ sensitivity of BNF,
117 particularly with incubation experiments. To improve mechanistic models of N
118 biogeochemistry, we propose a simple theoretical framework based on ammonium
119 transporter kinetics to link ambient porewater NH₄⁺ concentrations to BNF activity.

120 **Material and Methods**

121 *Culture conditions*

122 *Desulfovibrio vulgaris* var. *Hildenborough* (ATCC 29579), (Heidelberg et al., 2004) was
123 grown anaerobically in minimal diazotrophic media for sulfate reducers using a recipe

124 modified from Sim et al., 2013 in 27 mL Balch tubes (10 mL media) or 160 mL serum vial (50
125 mL media) with 20 mm butyl rubber septum stoppers (Bellco glass, Vineland, NJ, USA).
126 Medium modifications include the use of $0.07\text{g}\cdot\text{L}^{-1}$ ascorbate in place of titanium citrate as
127 the reductant and the omission of tungstate from the trace metal mix. Media was prepared
128 using standard anoxic procedures and a glovebox (Coy Laboratories, Grass Lake, MI, USA).
129 Resazurin ($1\text{mg}\cdot\text{L}^{-1}$) was used to monitor shifts in the redox potential of the medium during
130 our experiments. Sulfate (Na_2SO_4) was provided as an electron acceptor at 30 mM. Pyruvate
131 or sodium lactate (30 mM), used as the carbon and electron sources, were the growth
132 limiting nutrients. Sterilization was performed by autoclaving individual tubes for a minimum
133 of 15 min at 120°C . The final pH of the media was 7.3 ± 0.1 . Cells were grown at 30°C in the
134 dark, with tubes placed obliquely in an orbital shaker at a constant agitation speed of 130
135 rpm. *Clostridium pasteurianum* strain W5 was obtained from the DSMZ (German Collection
136 of Microorganisms and Cell Cultures, Braunschweig, Germany). The cells were grown in a
137 diazotrophic media with sucrose as the fermentative substrate as described in Westlake &
138 Wilson, 1959, in 27 mL Balch tubes (10 mL culture) sealed with 20 mm butyl rubber stoppers
139 (Bellco glass, Vineland, NJ, USA) and aluminum seals. Media tubes were sterilized by
140 autoclaving at 121°C for 45 minutes. Final pH of the media was 6.8. Cells were grown at
141 30°C in the dark, with constant orbital shaking at 100 rpm. Culture cell density was followed
142 by turbidimetry at OD 600 nm using a Thermo Fisher Scientific (Waltham, MA, USA)
143 GENESYS spectrophotometer equipped with a tube holder. Anoxic transfer of NH_4^+ as
144 ammonium chloride was accomplished using syringes and needles from 10- to 100-fold
145 stock solutions prepared in culture media.

146 *Slurry incubations of salt marsh sediments.*

147 Samples of salt marsh sediments (Table 1) were collected from Barnegat Bay in New Jersey
148 (denoted here as “NJ” saltmarsh, Lat: 40.031319, Long: -74.080609), the Sippewissett Salt
149 Marsh in Massachusetts (denoted here as “MA” saltmarsh, Lat: 41.590533, Long: -
150 70.639711) and from Great Bay in New Hampshire (denoted here as “NH” saltmarsh, Lat:

151 43.125, Long: -70.868). Sediments were kept at 4°C in the dark until being processed in the
152 laboratory. To determine sediment BNF sensitivity to NH_4^+ , 20 ± 1 g of wet sediment was
153 introduced in a 260 mL serum bottle and acclimated in an anoxic glove bag (2% H_2 98% N_2)
154 overnight for each incubation. On the day of the experiment, 80 mL of SRB minimal media
155 (described above) containing 30 mM lactate and 30mM SO_4^{2-} was added to each sample
156 prior to sealing the bottle. Each experiment had 10 replicates for each condition (NJ, n = 2;
157 NH and MA, n = 4) where ambient NH_4^+ concentrations and BNF activity (^{15}N and Acetylene
158 Reduction Activity, see methods below) were measured simultaneously. Samples were
159 incubated in the dark in an orbital shaker at 30 °C (ARA) and 26 °C (^{15}N) with constant
160 agitation (100 rpm). Six of the ten sediment samples assayed by ^{15}N received initial addition
161 of ammonium (~300 μM final concentration) before starting the experiments. After the initial
162 onset of BNF, we added NH_4^+ (~300 μM final concentration) in all but two samples (ARA,
163 NJ).

164 *Enrichment of sulfate-reducing bacteria*

165 Small amounts of sediment (~1 g) from the Barnegat Bay salt marsh were introduced into 60
166 mL serum bottles containing SRB-minimum media (prepared as described above). Initial
167 enrichments were sequentially transferred into fresh DIN-free media at least 6 times before
168 BNF sensitivity experiments. SRBB1 and SRBB2 enrichment cultures were grown under the
169 same conditions as strain *DvH*. Identity and purity of the enrichment consortia (NCBI
170 accessions will be added upon acceptance of the manuscript) were determined using 16S
171 rRNA and *nifH* genes.

172 *Evaluation of N_2 fixation activity.*

173 To avoid its inhibitory effects, a lower acetylene concentration (~ 2.5 % instead of 10%) than
174 typically used in the traditional Acetylene Reduction Assay (ARA) (Hardy et al., 1968) was
175 employed to assess changes in BNF activity by *DvH* and *Cp* cultures and sulfate-reducing
176 sediments. An experiment was started when culture at the beginning of exponential growth

177 (OD₆₀₀ ~ 0.09 for *DvH* and ~ 0.1 for *Cp*, Supplementary Figs. S3 and S4) by replacing ~
178 2.5 % of the total headspace (2.4-2.7%, depending on vessel volume) with 100% acetylene
179 generated anaerobically with N₂ background in a serum bottle from technical grade calcium
180 carbide (Sigma Aldrich, St Louis, MO, USA). At each time point, 1-3 mL of the headspace
181 was exchanged with the same volume of ~2.5% acetylene in N₂ and stored in a 3 mL
182 Exetainer ® vial (Labco, Lampeter, UK). Acetylene Reduction (AR) activity was evaluated by
183 measuring ethylene concentration in the headspace at different times using a Shimadzu
184 (Kyoto, Japan) 8A GC-FID as previously described (Bellenger et al., 2011). Results were
185 corrected for the sequential dilution of the headspace during resampling.

186 Direct nitrogen fixation activity was determined by measuring ¹⁵N incorporation into biomass
187 from ³⁰N₂ (Montoya et al., 1996). Briefly, the ¹⁵N tracer experiment was started by replacing
188 20% of the headspace and liquid phase with ³⁰N₂ gas (98%+ v/v, Cambridge Isotope
189 laboratories, Andover, MA, USA) and media equilibrated with ³⁰N₂ gas, respectively (Mohr et
190 al., 2010). At each time point, 3-4 mL of sediment slurry or cell culture was sampled and
191 centrifuged at 8000 rpm. Supernatant was filtered and used for NH₄⁺ measurement (see
192 below) and solid samples were stored at -20°C until further processing. Solid sediments
193 samples were then dried and weighed, and a known amount was sent for ¹⁵N and ¹³C
194 analyses at UC Davis Stable Isotopes Facility (<https://stableisotopefacility.ucdavis.edu>).

195 *Measurement of ammonium concentration.*

196 At every time point for assessing BNF activity by ARA or the ¹⁵N tracer method, 1-3mL of
197 supernatant was removed from the incubation and filter-sterilized (0.2 µm hydrophilic PTFE
198 or PES syringe filters, Agilent Technologies and MilliporeSigma, respectively). Filtered
199 samples, procedural blanks, and freshly prepared NH₄⁺ chloride standards (0.8 µM - 0.1 M)
200 for NH₄⁺ analysis were then stored at -20°C until further processing. Ammonium was
201 measured by fluorescence using the o-phthalaldehyde (OPA) method (Holmes et al., 1999).
202 Under our conditions, uncertainty for [NH₄⁺] in the range of 0-10 µM was estimated using

203 duplicate measurements over 3 different days (n=20) and found to be 1.3 μM . Several
204 filtered supernatant aliquots representing several timepoints sampled from five sediment
205 incubations assessed by ARA (#4, #6, #7, #9, #10) after NH_4^+ addition exhibited irregular
206 coloration (red-black instead of yellow) during the OPA procedure, even after 8-fold dilution
207 (Supplementary Fig. S2). After careful examination (see Supplementary Material Sup.
208 Discussion), these measurements (highlighted with red stars in Fig. 3 and Supplementary
209 Fig. S5) were disregarded for the purpose of this study. To determine the NH_4^+ threshold for
210 BNF inhibition (see Fig. 3), several NH_4^+ concentrations were averaged over two time-points
211 to link BNF rate and NH_4^+ concentration, without significant influence on the statistical
212 determination of $[\text{NH}_4^+]_{95\%}$ threshold value estimates.

213 Review of porewater ammonium concentration in sediments.

214 To estimate the extent to which sediment porewater ammonium concentrations reach the
215 ammonium threshold for BNF inhibition at the global scale, we extracted porewater
216 ammonium concentrations and depth gradients from 26 studies representing 5 continents
217 (Europe, North America, South America, Asia, and Oceania). We reviewed all benthic
218 references included in Knapp et al. 2012, as well as several references reporting BNF at
219 high $[\text{NH}_4^+]$. We further identified more recent publications using a keyword search in Google
220 Scholar, searching for "ammonium concentration sediments pore water coastal" and filtering
221 the results to include studies published after 2012 (Supplementary Table S1). Papers were
222 manually inspected, and ammonium concentrations when present were collected from tables
223 or estimated from direct graphic reading when no tabulated values were available (~ 10% or
224 5 μM of reading uncertainty, whichever was larger). For each sediment dataset, we derived
225 the general shape of the depth gradient of porewater ammonium (*i.e.*, depth and $[\text{NH}_4^+]$
226 values were extracted at initial, break in slope, plateau, and maximal measurement depths).
227 For the value of ammonium concentration at 0 cm (sediment/water interface), the value
228 reported in the study, $[\text{NH}_4^+]$ of the overlying water, or 0 μM was used, in this order of
229 preference. We then applied a linear interpolation to estimate the depth at which the

230 porewater concentration was equal to our threshold (*i.e.* threshold depth). When data were
231 presented as an average value for the whole sample or sediment core, the average
232 porewater [NH₄⁺] was attributed to the average depth (*i.e.*, half the maximal depth of
233 sampling) before interpolation.

234 *Extraction and analysis of nucleic acid sequence from salt marsh sediments.*

235 At the end of the ARA and ¹⁵N incubations, 3 mL of slurry was removed from the samples,
236 centrifuged at 5000 g, resuspended in LifeGuard® Soil Preservation solution (Qiagen,
237 Germantown, MD, USA) and stored at -20°C. DNA and RNA extraction were conducted
238 using the RNEasy PowerSoil® Total RNA and DNA elution kit (Invitrogen, Carlsbad, CA,
239 USA) following the recommendation of the supplier and extracts were stored at -80°C.
240 Nucleic acid purity was assessed using NanoDrop (Thermo Fisher Scientific) and Qubit®
241 (Thermo Fisher Scientific) measurements. RNA samples were converted into cDNA using
242 the SuperScript ® IV First Strand kit (Invitrogen) following the recommendation of the
243 supplier. Nested PCR amplification of *nifH* genes from DNA and cDNA were conducted in
244 triplicate according to the modified protocol of Zehr et al., 1998 from Jayakumar et al., 2017.
245 Amplification was verified by gel electrophoresis and amplicons from cDNA were pooled and
246 sent with total DNA extract for *nifH* and 16S rRNA gene sequencing using bTEFAP ® and
247 Illumina MiSeq300 at the MRDNA ® facility (Shallowater, TX, USA). 16S rRNA genes were
248 sequenced using 515f/806r primer pair targeting the V4 region (Caporaso et al., 2012), and
249 *nifH* genes were sequenced with the nifH1/nifH2 primer pair (Zehr & McReynolds, 1989).
250 The commercial in-house data processing pipeline at MRDNA® was used to process the
251 sequence data and cluster OTUs (97% similarity threshold). OTUs were taxonomically
252 classified against a curated database derived from the Ribosomal Database Project Release
253 11 (RDPII) for the 16S rRNA gene and the NCBI non-redundant nucleotide sequences
254 database for *nifH*.

255 We pruned the sequence datasets to retain only OTUs with absolute abundance > 1 000
256 counts and relative abundance > 0.2%. The top 500 *nifH* gene OTUs and the pruned
257 transcript OTUs (n=55) from ARA and ¹⁵N incubations, as well as *nifH* gene OTUs (n=46)
258 from our two salt marsh enrichments SRBB1 and SRBB2 were aligned against a
259 representative (*i.e.*, all major *nifH* groups represented) subset (n=152) of *nifH* database
260 recently curated in a deep sea sediment study (Kapili et al., 2020). Aligned sequences (see
261 Fig. 4A) were then separated into gene (after pruning, n=59) and transcript datasets to build
262 individual maximum-likelihood phylogenetic trees using FastTree (v2.1.11, GTR+CAT model,
263 1,000 resamples, Price et al., 2010). Data processing and visualizations were conducted
264 using R Studio (v1.3.1056) and R (v4.0.3) using the *phyloseq* (v.1.32.0) (McMurdie &
265 Holmes, 2013) and *ggtree* (v2.2.4) packages. Hierarchical clustering (*stat* v4.0.3, method
266 Ward.D2) was conducted on *clr*-transformed relative abundance data (Gloor et al., 2017)
267 using the package *compositions* (v2.0-0) (van den Boogaart & Tolosana-Delgado, 2008).
268 Canonical Analysis of Principal coordinate (CAP, 45) were performed on OTUs abundance
269 data using Bray-Curtis dissimilarity, and a Redundancy Analysis (RDA as implemented in
270 *vegan* v2.5-6, Oksanen et al., 2019) was conducted on normalized geochemical data. It is
271 worth noting that we were still able to find *nifH* sequences in the reagent blank control,
272 indicating contamination (Goto et al., 2005; Zehr et al., 2003) or cross-contamination
273 between samples during extraction or sequencing. In particular, two-three sediment slurry
274 samples, characterized by low DNA concentration, purity, and a low number of sequences (<
275 50 000 counts, Fig. 4B), cluster with our control sequence data, indicating they might be
276 disproportionately affected by contamination (purple box in Fig. 4B top panel and Fig. 5B).

277

278 **Results**

279 *Growth rates and yields of Desulfovibrio vulgaris and Clostridium pasteurianum under*
280 *diazotrophic and ammoniotrophic conditions*

281 We compared the growth of the two models anaerobic diazotrophs *D. vulgaris* var
282 Hildenborough (strain *DvH*) and *Clostridium pasteurianum* (*Cp*) under fully diazotrophic and
283 NH_4^+ replete conditions (Fig. 1A and B). For *DvH*, as expected for diazotrophs, including
284 SRB (Lespinat et al., 1987), diazotrophic growth ($\mu_{\text{N}_2} = 0.046 \pm 0.005 \text{ h}^{-1}$, SE n=3) was much
285 slower (~ 2-fold) than NH_4^+ replete growth ($\mu_{\text{NH}_4^+} = 0.10 \pm 0.004 \text{ h}^{-1}$, SE, n=3), compatible
286 with the typically higher energetic costs of BNF compared to NH_4^+ usage for N anabolism
287 (Inomura et al., 2017). Biomass yields ($\text{OD}_{\text{Max,NH}_4^+} = 0.82 \pm 0.02$ vs. $\text{OD}_{\text{Max,N}_2} = 0.39 \pm 0.01$,
288 SE n=3, Fig. 1A) also support this interpretation. Growth at sub-replete initial NH_4^+
289 concentrations under our culture conditions (e.g., $[\text{NH}_4^+] = 500 \mu\text{M}$, 30 mM pyruvate, 30 mM
290 sulfate, Fig. 1A) showed clear biphasic growth, with a first exponential growth phase ($\mu =$
291 0.094 h^{-1}), a second lag phase of ~ 50 h, and a second short exponential growth phase ($\mu \sim$
292 0.007 h^{-1}), all being consistent with a transition from ammoniotrophic to diazotrophic growth
293 as medium NH_4^+ becomes depleted. Accordingly, no BNF activity as measured by ethylene
294 production by ARA was detected during ammoniotrophic growth in similar experiments (data
295 not shown).

296 *Clostridium pasteurianum* grown fermentatively on sucrose exhibited a shorter lag-phase
297 than *DvH* regardless of N status (5h for *Cp* vs 50h for *DvH*, Fig. 1B). *Clostridium*
298 *pasteurianum* grew 1.5-fold slower under diazotrophic conditions ($\mu_{\text{N}_2} = 0.238 \pm 0.006 \text{ h}^{-1}$, SE
299 n=3) (Fig. 1B) than during NH_4^+ replete growth ($\mu_{\text{NH}_4^+} = 0.358 \pm 0.002 \text{ h}^{-1}$, SE n=3). While the
300 slower growth and lower biomass yield of diazotrophy relative to ammoniotrophy by *Cp*
301 ($\text{OD}_{\text{Max,NH}_4^+} = 1.6 \pm 0.02$ vs. $\text{OD}_{\text{Max,N}_2} = 1.3 \pm 0.01$, SE n=3, Fig. 1B) demonstrate the higher
302 metabolic cost of N acquisition by BNF during fermentative growth, the differences are not
303 as large as observed for sulfate reducing *DvH*. The faster growth of *Cp* relative to *DvH*
304 corresponded with a very fast and barely measurable transition (~ 1 h for *Cp* vs 50 h *DvH*)
305 between ammoniotrophic and diazotrophic growth regimes, which was induced by initial
306 growth on sub-replete ammonium levels (Fig. 1B).

307 *BNF dependency on timing and concentration of ammonium additions to N₂-fixing pure*
308 *cultures*

309 To study the response of BNF to extracellular NH₄⁺, we performed NH₄⁺ addition
310 experiments on the slower growing *DvH* acclimated to fully N₂-fixing conditions (no NH₄⁺
311 addition, Fig. 1C) and tracked BNF using acetylene reduction assays (ARAs) with a 2.5%
312 acetylene headspace concentration (see Material and Methods). This concentration of
313 acetylene decreased but did not prevent the growth of *DvH* or *Cp* (Supplementary Figs. S3A
314 and S4A). BNF generally decreased within the 26 h after the addition of varying
315 concentrations of NH₄⁺ (10 – 3,000 μM) (Fig. 1C). However, the response of *DvH* BNF to
316 NH₄⁺ addition was highly dependent on both the concentration of added NH₄⁺ and the timing
317 of sampling after the addition, as has been found for the DIN sensitivity of other diazotrophs
318 (Drozd et al., 1972; Holl & Montoya, 2005).

319 To better understand the relative contributions of BNF and external NH₄⁺ to fulfilling cellular
320 N growth demands, we calculated the contribution of BNF to new biomass production (Fig.
321 1D) using the quantity of newly fixed N (derived from ARA activity), the increase in biomass
322 (measured as OD₆₀₀), and the quantity of N required to produce 1 OD equivalent of biomass
323 under N₂-fixing and NH₄⁺-utilizing conditions (Supplementary Methods S1). Figure 1C shows
324 the reliance on BNF to fulfill N demands depends on the amount of added NH₄⁺ and that
325 higher initial spike concentrations result in longer times for the resumption of BNF. At the
326 highest NH₄⁺ addition (3,000 μM), the contribution of BNF to cellular N supply dropped to 0
327 in less than six hours and never resumed, showing that the amount of added NH₄⁺ was more
328 than sufficient for the culture to complete growth under our conditions. Lower concentrations
329 of added NH₄⁺ (< 300 μM) led to an initial drop in BNF followed by a slow increase back to
330 ~100% of its contribution to N supply, indicating that cells fully assimilated the added NH₄⁺ to
331 support their growth. At the first sampling time point (3 h), addition of NH₄⁺ > 100 μM showed
332 similarly low residual contributions of BNF to growth (~10-15% of initial BNF activity, Fig. 1C
333 and D) implying that at these concentrations the time to the onset of BNF inhibition (T_R, *i.e.*

334 the time necessary for the cell to sense external NH_4^+ , modify its metabolism, and
335 significantly decrease BNF), is independent of NH_4^+ concentration. By extrapolating the
336 contribution of BNF to the time space, and assuming a drastic shift from nitrogen fixation to
337 NH_4^+ uptake at T_R , 100% BNF contribution continues for a maximum of 15% of 3 h = 30 min
338 after addition, then drops to 0%. Hence, in liquid culture of *DvH*, $T_R < \sim 30$ min. In the first 3
339 h, residual contributions of BNF to cell growth were higher for NH_4^+ additions $< 100 \mu\text{M}$ than
340 when $> 100 \mu\text{M}$ was added (e.g., 50% at $30 \mu\text{M}$ vs. 15% at $100 \mu\text{M}$), and we found no
341 inhibition at the lowest level of added NH_4^+ ($10 \mu\text{M}$), suggesting that T_R might be
342 concentration-dependent at low external NH_4^+ concentrations ($10 - 30 \mu\text{M}$).

343 *Ammonium sensitivity of BNF in batch cultures of sulfate-reducing and fermenting bacteria*

344 To determine the ambient NH_4^+ concentrations associated with changes in BNF activity, we
345 simultaneously measured BNF activity and medium $[\text{NH}_4^+]$ in NH_4^+ addition experiments with
346 *DvH*, (Fig. 2A and Supplementary Fig. S3), *Cp* (Fig. 2B and Supplementary Fig. S4), and
347 two sulfate-reducing microbial enrichment consortia SRBB1 and SRBB2 dominated by
348 *Desulfovibrio desulfuricans* sp. (Fig. 2C and Supplementary Fig. S5). Biological N fixation
349 rates in all culture incubations decreased after NH_4^+ was added to cultures growing in fully
350 diazotrophic conditions (Fig. 2A-C, Supplementary Fig. S3-S5). We did not find any evidence
351 of BNF activity in *DvH* and SRBBs enrichment when measured ambient NH_4^+ concentrations
352 were $> 2 \mu\text{M}$ (Fig. 2A and C, Supplementary Fig. S3 and S5). Consistent with our previous
353 experiments with *DvH* (Fig. 1D), interpolations of BNF rates before and after NH_4^+ addition
354 for *DvH*, SRBB2, and *Cp* (dashed lines, Fig. 2A-C), showed noticeable inhibition of BNF in
355 all cultures within 0.5 - 3 h post-addition. After ammonium addition, bacterial uptake of NH_4^+
356 for growth led to the removal of $> 400 \mu\text{M}$ NH_4^+ in less than 30 h for *DvH* (max uptake rate \sim
357 $500 \mu\text{M}_{\text{NH}_4^+} \cdot \text{OD}^{-1} \cdot \text{h}^{-1}$) and in less than 4 h for *Cp* (see Supplementary Figs. S3-S5). Full
358 removal of NH_4^+ coincides with the recommencement of BNF (e.g., resumption of ethylene
359 production in Fig. 2A-C).

360 *Ammonium sensitivity of BNF in sulfate-reducing salt marsh sediments*

361 To evaluate the sensitivity of BNF by benthic organisms to NH_4^+ under conditions that are
362 more representative of natural environments, we performed incubation experiments on
363 slurries of salt marsh sediments collected from Barnegat Bay (NJ), Sippewissett Bay (MA),
364 and Great Bay (NH) (Fig. 2D-F, Supplementary Figs. S6 and S7). We evaluated BNF using
365 both ARA and ^{15}N tracer methods to account for possible artifacts associated with the use of
366 acetylene to estimate BNF (Fulweiler et al., 2015; Payne & Grant, 1982). For both ARA and
367 $^{15}\text{N}_2$ tracer incubations (10 incubations per method), we observed the onset of BNF only
368 after the levels of dissolved NH_4^+ initially present in slurries decreased drastically (to $[\text{NH}_4^+] <$
369 $20 \mu\text{M}$) (Fig. 2D-F, Supplementary Figs. S6 and S7). In the $^{15}\text{N}_2$ tracer incubations, five of
370 ten samples (Supplementary Fig. S7 #3, #5, #6, #7, and #9) showed a decrease in ^{15}N
371 incorporation into organic matter before NH_4^+ addition, and two of them completely stopped
372 incorporation of ^{15}N (Supplementary Fig. S7 #3 and #9). In parallel, NH_4^+ concentrations
373 slightly increased from $< 8 \mu\text{M}$ to levels around $10\text{-}18 \mu\text{M}$ in several samples prior to NH_4^+
374 addition (Supplementary Fig. S7 #3, #4, #5, and #9), suggesting the presence of some
375 endogenic NH_4^+ production within our experiments.

376 Similar to our results with cultured diazotrophs, NH_4^+ additions (e.g., target $[\text{NH}_4^+] \sim 300 \mu\text{M}$,
377 indicated with arrow, Fig. 2E and F) to actively fixing samples coincided with a fast decrease
378 in ethylene production to a complete stop in less than $\sim 3 \text{ h}$ in all our samples ($n=20$). For
379 four of the eight ARA-assayed sediment samples (two each from NH and MA salt marshes)
380 spiked with NH_4^+ , BNF responded normally to NH_4^+ , *i.e.* BNF rates resumed to pre-addition
381 values once ambient NH_4^+ was drawn down to near background levels ($[\text{NH}_4^+] < 10 \mu\text{M}$, Fig.
382 2E, Supplementary Fig. S6), likely due to assimilatory or dissimilatory biological activities.
383 The post-addition results from the other four of eight ARA samples with NH_4^+ added (two
384 each from NH and MA salt marshes) were excluded because of dubious OPA
385 measurements of $[\text{NH}_4^+]$ (see Methods and Supplementary Discussion). Importantly, none of
386 the 10 sediment incubations assayed using the ^{15}N tracer method, which directly reflects

387 BNF activity, showed any evidence of a resumption of BNF activity after NH_4^+ addition, and
388 post-addition NH_4^+ concentrations never decreased below 50 μM (Fig. 2F and
389 Supplementary Fig. S7). We note that the general decrease in $\delta^{15}\text{N}$ of OM in these samples
390 after NH_4^+ addition is consistent with the assimilation of the unlabeled NH_4^+ added to the
391 incubation, which could also impact the timing and sensitivity of the method to detect BNF.

392 *Determination of NH_4^+ threshold for benthic BNF*

393 Fast removal of ammonium from media due to high metabolic activity (e.g., growth) of the
394 samples, uncertainties on the ethylene concentration in headspace due to sequential dilution
395 during sampling, and variations in the timing for the BNF inhibition response after NH_4^+
396 addition all preclude a direct measurement of the exact ammonium concentration at which
397 BNF stops. To obtain a best estimate of the threshold for ammonium inhibition of BNF for
398 each type of experiment, we used the 95th percentile of all measured NH_4^+ concentrations
399 where BNF was present (before NH_4^+ addition) or resumed (after NH_4^+ addition) as a robust
400 estimate for the threshold NH_4^+ concentration that induce changes in BNF activity (Fig. 3,
401 number of datapoints for cultures in liquid media: $n=10$, ARA sediment slurries: $n=52$, and
402 ^{15}N tracer sediment slurries: $n=20$). For each sample, significant BNF activity corresponds to
403 BNF activity > 5% of the maximal BNF activity. Results from *Cp* were not included in this
404 analysis as we could not verify the complete inhibition followed by resumption of BNF in any
405 of our replicates (Fig. 2B and Supplementary Fig. S4). This is likely due to the removal of
406 NH_4^+ faster being than the response time for complete BNF inhibition by the fast-growing *Cp*
407 cultures, as well as by our limited sampling frequency.

408 Threshold values of $[\text{NH}_4^+]$ are < 2 μM (average \pm SD of $0.7 \pm 0.7 \mu\text{M}$) for all sulfate-
409 reducing liquid media cultures (*DvH* and SRBB1 and SRBB2, Fig. 3A), consistent with
410 values obtained for other cultured diazotrophs (Dekaezemacker & Bonnet, 2011; Sweet &
411 Burris, 1981) and oligotrophic pelagic BNF (Knapp, 2012). We note that the actual threshold
412 value is likely lower than our reported estimate of 2 μM because of the precision of the NH_4^+

413 measurement in our conditions (reproducibility_{0-10 μ M} ~ 1 μ M). While the fast growth, fast
414 removal of ammonium, and our insufficient sampling frequency does not allow for an
415 accurate determination of NH_4^+ threshold in *Cp*, we estimate that its value to be anywhere
416 between 0 and 20 μ M, as evidenced by BNF slow-down ~3 h post-ammonium addition and
417 its recommencement ~10 hr post-addition (Fig. 2B, ammonium at t~ 8h vs 14 hr). Threshold
418 values of ~ 7 μ M and ~ 11 μ M were found for BNF in slurries assessed by ARA and ^{15}N
419 tracer methods, respectively (Fig. 3B and C). This value is in good agreement with similar
420 experiments performed with deep-sea sediments (< 25 μ M) (Dekas et al., 2018). All these
421 direct measurements of NH_4^+ thresholds are consistent with calculations of the external
422 $[\text{NH}_4^+]$ at which BNF resumes in experiments with *DvH* (Fig. 1C and D) that account for the
423 drawdown of external NH_4^+ contributing to biomass growth ($[\text{NH}_4^+]_{\text{calculated}} < 23 \mu\text{M}$,
424 Supplementary Methods S2 and Fig. S8).

425 *Diazotrophic community in enrichment cultures and slurry experiments*

426 In both SRBB1 and SRBB2, *nifH* taxonomic diversity was dominated by several
427 operational taxonomic units (OTUs) closely related to the SRB *Desulfovibrio desulfuricans*.
428 SRBB1 showed the additional presence of an OTU closely related to the genus *Clostridium*
429 (Supplementary Fig. S1A). Other OTUs (e.g., *Desulfovibrio fructosovorans*, *Azotobacter*
430 *vinelandii*, and *Pelobacter carbinolicus*) were found in low abundance (<1% of total *nifH*
431 genes). The 16S rRNA gene diversity confirmed the dominance of *Desulfovibrio* and
432 *Clostridium* species in the enrichments (Supplementary Fig. S1B).

433 To determine the diazotrophic community that developed in our sediment incubations
434 and compare them to those in other benthic environments, we sequenced *nifH*, which
435 encodes a component of the Mo-nitrogenase and is the most common phylogenetic marker
436 used in studies of diazotroph diversity (Fig. 4). Analysis of *nifH* gene diversity in DNA
437 extracted from sediments at the end of incubation (5 days) revealed the dominance of
438 sequences related to those from delta-proteobacteria, particularly sulfate-reducing genera

439 (closely related to *Desulfovibrio desulfuricans*, *D. salexigens*, *Desulfatibacillum alkenivorans*,
440 *Desulfuromonas acetoxidans*), as well as other anaerobic bacteria (e.g. *Pelobacter*
441 *carbinolicus* and *Marichromatium purpuratum*). These diazotrophic taxa have also been
442 identified in other salt marshes (Burns et al., 2002; Steppe & Paerl, 2005), and in estuarine
443 (Burns et al., 2002; Newell, Pritchard, et al., 2016), and deep-sea sediments (Gier et al.,
444 2016; Kapili et al., 2020). Examination of *nifH* transcript diversity at the end of incubations
445 showed similar results suggesting that the putative diazotrophs identified based on *nifH* gene
446 diversity are likely active during our incubation (Fig. 4A and Supplementary Fig. S9).

447 *Relationship between nitrogenase activity and sediment biogeochemical characteristics*

448 The richness of *nifH* transcripts (expressed as observed number of OTUs, Fig. 5A) was
449 similar at the end of incubations, even in treatments exhibiting high final concentrations of
450 NH_4^+ (> 100 μM) and no $^{15}\text{N}_2$ incorporation or acetylene reduction activity in the previous 20-
451 30 h (Fig. 2, symbol gradient shade in Fig. 5A, Supplementary Fig. S6 and S7). Biological N
452 fixation activity at the end of incubation was only detected for NH_4^+ concentrations less than
453 ~ 20 μM . This strongly supports a post-transcriptional inhibition of nitrogenase activity by
454 NH_4^+ and slow turnover of *nifH* transcripts in our incubations.

455 Hierarchical clustering of our samples and Canonical Analysis of Principal Coordinates on
456 the OTU abundance data (Hellinger transformation) indicates that geographical origin (NJ,
457 MA, and NH) rather than the type of incubation (i.e., BNF assayed by ARA or ^{15}N) best
458 explains sediment *nifH* composition (see colored boxes in top panel Fig. 4B, Fig. 5B, and
459 Supplementary Fig. S10). We identified several OTUs showing significant differences in
460 relative abundance between ARA and ^{15}N incubation conditions based on 16S rRNA gene
461 diversity, but not for *nifH* gene and transcript abundance (Supplementary Fig. S10C). Net
462 NH_4^+ removal rates (as the balance between all processes that remove NH_4^+ minus the
463 potential release of NH_4^+ from sediments) are correlated with initial (pre-addition) NH_4^+

464 concentrations, and maximum BNF rates are positively correlated with sediment C:N ratios
465 (Fig. 5C).

466 *Literature review of benthic porewater ammonium concentrations*

467 To estimate the extent to which BNF can occur in benthic sediments (Fig. 6A), we combine
468 all data by transforming the ARA- and ¹⁵N-based results so that they are relative to the
469 maximum in each replicate ($(V_{\text{BNF,Max}} - V_{\text{BNF}}) / V_{\text{BNF,Max}}$). It allows us to derive a single
470 estimate of NH_4^+ threshold for BNF in sediments of $[\text{NH}_4^+]_{\text{threshold}} = 9 \mu\text{M}$ (Fig. 6B, n=72). We
471 then analyzed porewater ammonium concentration data from 26 studies including 151 sites
472 and more than 300 individual samples representing a diversity of benthic environments (Fig.
473 6C and D, SI Table S1). We estimate the fraction of global sediments where BNF might
474 occur by deriving the depth ('threshold depth', see Fig. 6A) at which published porewater
475 $[\text{NH}_4^+]$ equaled the threshold value of BNF inhibition of $\text{NH}_4^+ = 9 \mu\text{M}$ (Fig. 6C and D). The
476 median depth at which porewater ammonium reaches the threshold value is 0.3 cm (Fig. 6C,
477 average 0.65 cm, range 0 – 25 cm, n=151). In this review, ~ 87 % of the values collected
478 (based on individual cores, n=334) exceeded the $[\text{NH}_4^+]_{\text{threshold}}$ at depths deeper than 1 cm
479 below surface, and 95 % of values exceeded the threshold at depths of ~ 3 cm below
480 surface. Porewater $[\text{NH}_4^+]$ was lower than the threshold at any measured depth in only ~
481 0.1% of all individual cores (3 of 334). Results separated along the different benthic zones,
482 *i.e.*, tidal (< 4 m, n=64), sub-littoral (between 4 and 200 m, n=47), and bathyal (> 200 m,
483 n=40), are available in Supplementary Fig. S12.

484

485 **Discussion**

486 *Metabolic cost of BNF in anaerobic diazotrophs*

487 The metabolic cost of using BNF versus fixed N sources like ammonium to support growth
488 can yield insights on ecophysiology of microorganisms in nature. The substantively lower

489 growth rates and yields observed for diazotrophic versus ammoniotrophic growth of the
490 sulfate-reducer *DvH* (2-fold growth rate and yield) and the fermenter *Cp* (1.5-fold growth rate,
491 1.2-fold yield) indicate a significant metabolic cost of BNF as an N source in anaerobic
492 bacteria. The cost of BNF in diazotrophs that have metabolisms involving O₂ is even more
493 substantial given the additional energetic costs of protecting nitrogenase and other O₂-
494 sensitive BNF-related enzymes from oxidative damage (Großkopf & LaRoche, 2012;
495 Inomura et al., 2017) Collectively, the physiological data for anaerobic diazotrophs presented
496 here, as for other types of diazotrophs, support the paradigm of prevalent BNF in
497 environments with limiting amounts of fixed N.

498 *Ammonium threshold for BNF in diazotrophic bacteria and its relation to cellular N*
499 *metabolism*

500 Our results show that BNF activity in sulfate-reducing bacteria and sulfate-reducing
501 sediments is sensitive to fixed nitrogen (as NH₄⁺) at micromolar concentrations. This
502 conclusion does not appear to support the use of BNF as an important mechanism to
503 balance intracellular redox in ammonium-rich benthic systems, as previously hypothesized
504 (Tichi & Tabita, 2000). The onset of inhibition of BNF activity occurs for [NH₄⁺]_{threshold} < 2 μM
505 in liquid cultures of SRB; a slightly higher threshold of [NH₄⁺]_{threshold} < 11 μM was found in
506 slurry incubations. This is in good agreement with existing knowledge of the biochemistry
507 and metabolism of nitrogen fixers (Dekaezemacker & Bonnet, 2011; Hartmann et al., 1986;
508 Holl & Montoya, 2005; Kleiner, 1974; Ohki et al., 1991; Postgate & Kent, 1984). Our
509 threshold estimates are also consistent with early studies in salt-marsh sediments
510 ([NH₄⁺]_{threshold} < 33 μM) (Carpenter et al., 1978; Patriquin & Keddy, 1978), a recent studies of
511 BNF in deep-sea sediments ([NH₄⁺]_{threshold} < 25 μM) (Dekas et al., 2018), and pure culture
512 studies with *Desulfovibrio gigas* ([NH₄⁺]_{threshold} ~ 10 μM) (Kessler et al., 2001; Postgate &
513 Kent, 1984), *Rhodospirillum rubrum* (NH₄⁺]_{threshold} ~ 3-5 μM) (Sweet & Burris, 1981),
514 *Klebsiella oxytoca* ([NH₄⁺]_{threshold} < 10 μM) (Schreiber et al., 2016), *Methanococcus*
515 *maripaludis* ([NH₄⁺]_{threshold} < 25 μM) (Kessler et al., 2001), *Azotobacter vinelandii*

516 ($[\text{NH}_4^+]_{\text{threshold}} < 10 \mu\text{M}$) (Kleiner, 1974), and *Trichodesmium* ($[\text{NH}_4^+]_{\text{threshold}} < 10 \mu\text{M}$)
517 (Mulholland et al., 2001), and *Crocospaera watsonii* ($[\text{NH}_4^+]_{\text{threshold}} < 1 \mu\text{M}$)
518 (Dekaezemacker & Bonnet, 2011). While the ammonium threshold of BNF inhibition could
519 not be precisely estimated for the fermenter *Clostridium pasteurianum* ($[\text{NH}_4^+]_{\text{threshold}} < 20$
520 μM) due to rapid ammonium draw-down and low sampling frequency, the presence of
521 *Clostridia* relatives in the isolate SRBB1 (Supplementary Figs. S1 and S4) and Clostridia-like
522 *nifH* sequences in sediment slurries suggest a similarly high sensitivity.

523 Biological N fixation and NH_4^+ uptake are complementary N sources to cells. Nitrogenase
524 activity and gene regulation is controlled by intracellular NH_4^+ through the GS-GOGAT
525 systems. In most diazotrophs, low NH_4^+ supply to the cell leads to a decrease in intracellular
526 glutamine concentrations, turning on nitrogenase gene transcription and/or nitrogenase
527 protein activity through the PII signal-transduction cascade (Dixon & Kahn, 2004).
528 Conversely, sufficient NH_4^+ supply to the cell decreases BNF, either at the pre- or post-
529 transcriptional level. Cellular N and C metabolisms are coupled via the balance between α -
530 ketoglutarate, a metabolite of the TCA cycle, and glutamine (Huerigo & Dixon, 2015).
531 Extracellular N sources are acquired through the use of specific membrane transporters (e.g.,
532 AmtB for ammonium (Kleiner, 1985; Zheng et al., 2004)). Most other fixed-N sources, such
533 as NO_3^- , are first taken up and then intracellularly converted into ammonia by specific
534 enzymes (e.g., nitrate reductase) before being used anabolically. Assuming a Michaelis
535 Menten mechanism for NH_4^+ transport (Kuzyakov & Xu, 2013), we expect the affinity
536 constant of the NH_4^+ transporter to play a critical role in cellular sensing of and ability to grow
537 using external NH_4^+ (Javelle et al., 2004), thereby modulating internal N status and BNF
538 down-regulation (Fig. 6A). For example, at NH_4^+ concentrations $< K_m$ of the transporter, less
539 than 50% of NH_4^+ uptake activity can take place, reducing intracellular N concentrations and
540 inducing a metabolic cascade that ultimately leads to the onset of BNF activity. This
541 simplified framework would constrain the switch between ammoniotrophy and BNF or their
542 co-occurrence to NH_4^+ concentrations close to transporter K_m values (Schreiber et al., 2016).

543 In reviewing the literature, we found that the K_m values for AmtB, the most common NH_4^+
544 transport protein, in a variety of nitrogen fixers, range in value from approximately 1 to 20 μM
545 (Kleiner, 1985). These values are in good accordance with our experimental data and prior
546 literature which show BNF inhibition thresholds of 2-10 μM NH_4^+ . Given these estimates,
547 BNF activity in environment with high N loadings would not be unexpected when residual
548 dissolved NH_4^+ concentrations are $< 20 \mu\text{M}$ (Foster & Fulweiler, 2014).

549 *Timing of inhibition and regulation of nitrogenase in anaerobic diazotrophs*

550 We found that T_R , the time to the onset of BNF inhibition after NH_4^+ addition, was
551 concentration-independent at $[\text{NH}_4^+] > 100 \mu\text{M}$, and concentration-dependent at $[\text{NH}_4^+] < 30$
552 μM , in accordance with a Michaelis-Menten mechanism for NH_4^+ sensing. Within this
553 framework, the lowest addition of NH_4^+ in this study (10 μM), which led to the longest delay
554 (> 3 h) in BNF inhibition (see Fig. 1D), can be explained by a sub-maximal uptake of NH_4^+
555 leading to the delay in cellular metabolic response. The passive diffusion of ammonia
556 through cell membranes is not likely to be important as the pH of media was ~ 7 and rate of
557 removal was faster in the faster growing bacteria (i.e., *Cp*) than in *DvH*, indicating an active
558 process.

559 The relatively short-time response of BNF to NH_4^+ additions in both pure culture and slurry
560 incubations (0.5 - 3h, as estimated from BNF rate interpolations, Fig. 2) and mass balance
561 calculations in Fig. 1D) and the fast resumption of BNF activity upon depletion of the external
562 NH_4^+ pool indicates that the control of NH_4^+ over nitrogenase activity is most likely post-
563 transcriptional. This is also supported by the presence of multiple *nifH* mRNA from SRB
564 clades within incubations with $[\text{NH}_4^+] > 100 \mu\text{M}$ and no BNF activity. Boyd and co-workers
565 have suggested that post-transcriptional regulation arose during the evolutionary transition
566 from anaerobic to aerobic BNF as an early strategy of anaerobes for optimizing BNF activity
567 in fluctuating environments (Boyd et al., 2015). Pure culture studies on anaerobic organisms
568 (Heiniger & Harwood, 2015; Kessler et al., 2001; Masepohl et al., 2002) and field studies in

569 salt marsh sediments using methionine sulfoxide, an inhibitor of glutamine synthase, also
570 support this interpretation (Gandy & Yoch, 1988; Yoch & Whiting, 1986). The results of this
571 study, with frequent measurement of ammonium and BNF activity over the incubation period,
572 and the likely post-transcriptional nature of NH_4^+ inhibition of nitrogenase in anaerobic
573 systems, reiterates the need for higher time resolution flux measurements for better *in situ*
574 BNF estimates in natural environments.

575 Interestingly, there is a drastic difference between the long lag-phase (~ 20-50h) at the initial
576 onset of diazotrophy both in *DvH* cultures (without initial NH_4^+ and during the transition
577 between ammoniotrophy and diazotrophy) and in slurry incubations, and the rather rapid
578 inhibition and resumption of BNF following NH_4^+ removal in actively fixing samples (< 3h)
579 (Fig. 1C and Fig. 2). This suggests that SRB organisms living in environments with
580 fluctuating N concentrations close to the NH_4^+ threshold value might maintain an intracellular
581 nitrogenase pool that can help them quickly resume BNF activity should there be local NH_4^+
582 depletion. Interestingly, BNF in *Cp* cultures remained active for ~ 3 hr after NH_4^+ addition
583 while NH_4^+ in media was quickly removed. Consistent with this observation, Yoch and
584 Whiting, 1986, found that undisturbed sediments amended with mannose, a preferred
585 substrate of fermenting bacteria, took longer to inhibit BNF than when lactate, a substrate
586 favoring SRBs, was used as the amended C source. In addition, and in opposition to our
587 findings with SRB, only scarce *nifH* transcripts attributed to *Clostridia* were found at the end
588 of our incubation experiments compared to their general presence in our samples (Fig. 4 and
589 Supplementary Fig. S10), indicating that transcriptional regulation of the *nif* genes could be
590 more prominent in this strain. The data suggest that even though the ammonium threshold
591 between SRB and firmicutes is likely similar, the sensing mechanism or inhibition pathway
592 could slightly differ (Gandy & Yoch, 1988; Gordon et al., 1981; Postgate & Kent, 1984; Tubb
593 & Postgate, 1973). How these differences in regulatory pathways influence the adaptation
594 and competitiveness of these organisms in benthic systems remains to be investigated.

595

597 Consistent with previous studies of saltmarsh, estuarine, and carbonate mud sediments
598 (reviewed by Capone, 1988; see also Welsh et al., 1996), we find strong and consistent
599 inverse relationships between ambient ammonium and BNF activity. Our estimate of NH_4^+
600 threshold for BNF in sediments of $[\text{NH}_4^+]_{\text{threshold}} = 9 \mu\text{M}$ (Fig. 6B, $n=72$). This value is lower
601 than any previously reported value for BNF inhibition in sediments, and is consistent with a
602 very early assessment of *in-situ* BNF sensitivity to porewater NH_4^+ in *Spartina* marshes
603 ($[\text{NH}_4^+]_{\text{threshold}}$ between 3 and 33 μM) (Patriquin & Keddy, 1978) and recent estimates in deep-
604 sea sediments ($[\text{NH}_4^+]_{\text{threshold}} < 25 \mu\text{M}$) (Dekas et al., 2018).

605 The potential diazotrophic genera identified in our sediment slurry experiments overlap well
606 with those found in other benthic systems, from intertidal salt marshes (Burns et al., 2002;
607 Steppe & Paerl, 2005), and estuaries (0-20m water level) (Burns et al., 2002; Newell,
608 Pritchard, et al., 2016) to deep oceanic floor sediment (100-1000m) (Gier et al., 2015; Kapili
609 et al., 2020), with the dominance of *Desulfovibrionaceae*, *Desulfobulbaceae*, as well as some
610 Firmicutes species (see Fig. 4). We found evidence in several of our samples for the
611 presence and transcriptional activity of *Pelobacter carolinicus* and *Desulfuromonas*
612 *acetoxidans*, which have been identified in a recent study on the diazotrophic community of
613 deep sea sediments using ^{15}N -SIP-RNA to probe the identity of the dominant diazotrophs
614 (Kapili et al., 2020). The observation of similar microbiome composition indicates that our
615 threshold estimates likely represent the general response of SRBs and possibly of other
616 types of anaerobic N fixers present in benthic systems (e.g., potential fermenters in SRBB1
617 diazotroph enrichment, Supplementary Fig. S1).

618 *In situ* porewater $[\text{NH}_4^+]$ in most benthic sediments (Knapp, 2012) is usually higher than our
619 observed threshold ($> 10\text{-}20 \mu\text{M}$) and increases with depth (Metzger et al., 2019) (Fig. 6A).
620 Our review of porewater ammonium data from 26 studies, including 151 sites and more than
621 300 individual samples indicates that the median depth at which our threshold value was

622 reached is 0.3 cm below sediment surface (Fig. 6C, based on site, average 0.65 cm, range 0
623 – 25cm, n=151). Overall, in our review, ~ 87% of the values collected (based on individual
624 cores, n=334) were over our $[\text{NH}_4^+]_{\text{threshold}}$ at a depth greater than 1 cm, and 95% at depth of
625 ~ 3 cm. This analysis suggests that BNF rates in sediments are likely to be greatest at the
626 surface and decrease rapidly to zero. Diffusion of O_2 from the sediment-water interface into
627 deeper layers could further reduce the opportunity for BNF to occur.

628 The previously reported relatively high ammonium values associated with BNF inhibition, like
629 those reviewed in Capone 1988 (~200-300 μM) and Knapp et al 2012 (50-2,000 μM), were
630 likely due to long incubation times (> 24 hr), the fast depletion of porewater ammonium, and
631 the reporting of *in situ* porewater $[\text{NH}_4^+]$ rather than measurement of ambient $[\text{NH}_4^+]$ during
632 incubation. Consistent with our results, many studies that track the timeline of N fixation
633 show very little if any activity in the first ~ 24 - 48 hr of incubation in saltmarsh sediments
634 when roots were excluded (Patriquin & Keddy, 1978; Yoch & Whiting, 1986). In contrast, *in*
635 *situ* incubations of vegetated saltmarshes sediments (Yoch & Whiting, 1986) demonstrate
636 rapid onset of BNF and the highest activity was found with surface-washed living roots and
637 rhizome samples, and with C addition, indicating a predominant role of root-associated
638 microbes and available C (*i.e.*, carbon substrate amendment, root exudates).

639 Thus, our results, which are compatible with our knowledge of the regulation of diazotrophy
640 (Dixon & Kahn, 2004), suggest that the extent of natural BNF activity in benthic sediments
641 may be mostly limited to N-limited superficial regions of the sediments (top 1 cm, Fig. 6) and
642 highly productive environments like seagrass meadows and *Spartina* marshes. The
643 observation of BNF associated with live vegetation roots in *Spartina* marsh with high $[\text{NH}_4^+]$
644 (Yoch & Whiting, 1986) is likely explained by local zones around and within plant roots
645 (Kuzyakov & Xu, 2013) in which NH_4^+ is depleted by plant and microbial uptake to
646 concentrations below our threshold estimates.

647 Our findings do not contradict the traditional view of a relatively small contribution of benthic
648 systems to total marine BNF compared to pelagic new N sources. Early studies have
649 suggested benthic contributions to global marine BNF of ~ 15 Tg N (Capone, 1988; Capone
650 & Carpenter, 1982), ~10% of total BNF (Zhang et al., 2020). Most of this activity was then
651 attributed to shallow benthic environments, particularly vegetated and coral reef ecosystems.
652 Based on the recent findings of Dekas et al. 2017 and consistent with our analyses of
653 ammonium thresholds (Supplementary Fig.S12), it is possible that unvegetated sediments
654 from the deep sea could constitute a larger source of new N than previously thought. More
655 precise accounting of benthic BNF however requires additional measurements in these and
656 other benthic systems that account for several methodological challenges in measuring BNF,
657 which we discuss below.

658

659 *Current methodologies for BNF investigations in sediments*

660 Our results show that the timing of inhibition is a critical factor to consider when assessing
661 the sensitivity of BNF to ammonium as a fixed N source. Measurement of BNF activity
662 before the onset of the inhibition response would lead to the false conclusion that BNF in a
663 tested sample is not or little sensitive to ammonium. Conversely, it is particularly critical to
664 measure and report the evolution of $[\text{NH}_4^+]$ over time along or at the end of incubations, as
665 typical incubation times, which range from 8 hours to several days, are sufficient for pore
666 water $[\text{NH}_4^+] > 100 \mu\text{M}$ to become depleted to background NH_4^+ levels (below threshold for
667 BNF activation). This precaution is particularly important in closed and semi-closed vessel
668 experiments with high activity samples (e.g., experiments with carbon addition, high C:N
669 sediments, and pure cultures), where ammonium-supported growth would drastically
670 increase the biomass and lead to higher BNF rates after fixed N addition.

671 Our measurements show that the apparent NH_4^+ concentration required to stop BNF in slurry
672 experiments ($[\text{NH}_4^+] < 11 \mu\text{M}$, Fig. 3B and C) is roughly five times higher than in liquid media

673 experiments (*DvH* and SRBB enrichments, $[\text{NH}_4^+] < 2 \mu\text{M}$, Fig. 3A). It is probable that our
674 measurement of the NH_4^+ concentration threshold for BNF is higher in the sediment slurries
675 due to higher spatial and temporal heterogeneity. Small biogeochemically distinct zones, or
676 microniches, could originate from slow nutrient diffusion to hotspots of highly active biomass
677 in heterogenous sediments and lead to imbalanced macronutrient ratios (C or P excess
678 relative to N). Indeed, our results show an association between maximal BNF rate and high
679 C:N (Fig. 5C), and reports on the occurrence of BNF at high fixed N have been correlated
680 with high C:N ratios of sediments (Hou et al., 2018). We particularly expect microniche
681 formation to be favored at high cell densities when the requirement for N in a large
682 population of active cells could outpace the diffusion of porewater NH_4^+ through the solid
683 phase. These conditions would prevail at the end of our incubations (~4-5 d) when the
684 addition of NH_4^+ and of 30 mM lactate, a readily available source of carbon to SRBs, resulted
685 in a high density of biomass. In addition, the heterogeneity of organic matter in our samples
686 is suggested by the high variability of sample C and N composition (Table 1), and even
687 though agitation was constant during our experiment, we observed macroscopic clumping of
688 slurry material and vegetation debris throughout the incubation period. The threshold NH_4^+
689 concentration values reported here were obtained for a wide range of sediment chemical
690 and isotopic composition (*i.e.*, %C, %N, C:N, $\delta^{13}\text{C}$, and $\delta^{15}\text{N}$, see Table 1), suggesting that
691 our threshold value should be general and apply to many benthic environments.

692 It is important to note both here and in other studies, the presence of *nifH* genes and
693 transcripts do not provide definitive proof of BNF activity in anaerobic settings, as we found
694 evidence consistent with post-transcriptional BNF regulation in benthic SRBs. In addition,
695 prolonged incubation (5 days for ARA or $^{15}\text{N}_2$ uptake experiments) along with addition of
696 carbon and sulfur (lactate + sulfate) could have drastically altered the biogeochemical
697 conditions within our microcosms (buildup of H_2S , removal of nutrients) and selected for
698 diazotroph species different from those important in natural microbial assemblages. These
699 long incubation periods could also have led to other artifacts that directly interfered with our

700 study, such as the rapid drawdown of high *in situ* NH_4^+ and abnormal NH_4^+ measurements
701 with the OPA method (see Methods and Supplementary Fig. S2 and Supplementary
702 Discussion), which strongly affect interpretations on the sensitivity of BNF activity to NH_4^+
703 (Supplementary Fig. S6 #4, #6, #9 & #10). In this regards, the use of *in situ* measurements
704 (Yoch & Whiting, 1986) and of several existing (ARA, ^{15}N , MIMS) and newly developed
705 methodological approaches (Aoki & McGlathery, 2019) could help produce a more accurate
706 view of N cycling in sediments.

707 The use of high concentration of acetylene (~25% v/v) has been shown to influence the
708 microbiome (16S mRNA) of estuary sediment samples during short-term incubations (~ 7 h)
709 (Fulweiler et al., 2015). Indeed, we were able to identify changes in microbial composition
710 based on 16S rRNA genes at 2.5% acetylene over 5 days of incubation (Supplementary Fig.
711 S10C). However, there was no significant differences in the *nifH* gene or transcript diversity
712 (Fig. 5B and Supplementary Fig. S10A and B) or in the response of BNF to NH_4^+ addition
713 between ARA and $^{15}\text{N}_2$ tracer incubations (Fig. 3), indicating that the use of a sub-saturating
714 concentration of acetylene (2.5%v/v) did not interfere with our study. Indeed, estimates of
715 *DvH* growth inhibition under these low acetylene conditions ($\mu_{\text{C}_2\text{H}_2} = 0.01 \text{ h}^{-1}$ vs $\mu_{\text{ctrl}} = 0.016$
716 h^{-1} , 30-40% inhibition, Supplementary Fig. S3) is consistent with the flux of electron diverted
717 from N_2 reduction to produce ethylene during ARA, as evaluated by nitrogenase acetylene
718 saturation in the presence of dinitrogen ($K_{\text{mC}_2\text{H}_2} \sim 0.5\text{-}4 \text{ kPa}$, ~40-60% saturation) (Davis &
719 Wang, 1980). This is in agreement with a previous report of acetylene inhibition in sulfate-
720 reducing bacteria (Payne & Grant, 1982), where an acetylene concentration of 5-10% only
721 partially inhibited growth rate and yield. In addition, the presence and activity of
722 molybdenum-independent nitrogenases in sediment (McRose et al., 2017; Zhang et al.,
723 2016) could also influence BNF rate determinations and the overall N input budget in benthic
724 areas when the ARA method is used without ^{15}N calibration (Bellenger et al., 2020). Indeed,
725 in our experiments, the average R ratio (i.e., $\text{C}_2\text{H}_2 : \text{N}_2$ ratio of activity), calculated with the
726 highest BNF rate reached for each method was 2.3 (range 0.16 – 5.5, n=10), possibly

727 indicative of the presence of alternative nitrogenase. Finally, in a set of unsuccessful
728 experiments containing fresh salt marsh sediment from Barnegat Bay (n=6), overlying water,
729 and addition of lactate, we did not observe any BNF activity (as AR and ^{15}N incorporation)
730 over the course of one week and one month, respectively, even though *nifH* genes were
731 presumably present in these sediments before our incubation (Fig. 4B). These results
732 indicate that other factors, such as water quality, (micro-) nutrient availability, and the nature
733 of the dissolved organic matter also likely influence the *in-situ* activity.

734 **Conclusion**

735 In this study, we demonstrate that various sulfate-reducing bacteria, and very likely
736 fermenting clostridia, found in coastal sediments exhibit high sensitivity to NH_4^+ addition, with
737 a $[\text{NH}_4^+]$ threshold for BNF inhibition below 10 μM . To mechanistically link BNF inhibition and
738 external NH_4^+ concentrations, we propose a simple framework of cellular N metabolism
739 based on the affinity constant of the NH_4^+ transporter. The measured threshold is likely to
740 apply to several benthic systems as the different diazotrophic genera identified here are
741 similar to those described in sediments ranging from the deep sea to coasts. Analysis of
742 published porewater data suggests that the vast majority of $[\text{NH}_4^+]$ reported for sediments
743 sampled at 1 cm below the sediment water interface exceed the threshold for BNF inhibition.
744 The data are consistent with the existing framework for a relatively small contribution of
745 benthic systems to marine new N inputs. Apparent discrepancies between our results and
746 previous reports of low NH_4^+ sensitivity in benthic environments could be explained by
747 porewater NH_4^+ concentrations close to the threshold value, fast removal of porewater NH_4^+ ,
748 sediment heterogeneity, and by considering the timing necessary after addition of NH_4^+ for
749 inhibition to be recorded (e.g. 30 min – 3 h as found here). Our research provides new
750 mechanistic insights on the biogeochemistry of nitrogen input into marine ecosystems that
751 can help improve N cycling models and guide future measurement studies of benthic BNF.

752

753 **Acknowledgements**

754 This research was funded by grants from the Simons Foundation (award ID 622944 to
755 X.Z.), the Carbon Mitigation Initiative at Princeton University (to X.Z.), and a Simons
756 Foundation / Life Science Research Foundation Postdoctoral Fellowship (to R.D). We thank
757 the Barnegat Bay Foundation for aid in collecting salt marsh sediments, J. Wilmoth, C.
758 Rusley, E. Zimble, and A. Jayakumar for aid with molecular analyses, the laboratories of
759 B.W.Ward and D. Sigman for aid with DIN analyses, and members of the Zhang laboratory
760 for useful discussions. Katja Luxem is on the Science Advisory Committee for the Watershed
761 Institute (NJ, <https://thewatershed.org/>). The authors declare no other competing interests.

762 **Availability statement**

763 All the data used for this study are currently available in Supplementary Materials
764 (Supplementary Materials _Dataset). Upon manuscript acceptance, the dataset files will be
765 deposited to Figshare, all molecular datasets will be deposited on NCBI database, and the R
766 Markdown code and associated files to reproduce all figures will be deposited at GitHub.

767 **References:**

768 Anderson, M. J., & Willis, T. J. (2003). Canonical analysis of principal coordinates: A useful
769 method of constrained ordination for ecology. *Ecology*, *84*(2), 511–525.

770 [https://doi.org/10.1890/0012-9658\(2003\)084\[0511:CAOPCA\]2.0.CO;2](https://doi.org/10.1890/0012-9658(2003)084[0511:CAOPCA]2.0.CO;2)

771 Aoki, L. R., & McGlathery, K. J. (2019). High rate of N fixation in seagrass sediment
772 measured via a direct 30N₂ push-pull method. *Marine Ecology Progress Series*, *616*,
773 1–11. <https://doi.org/10.3354/meps12961>

774 Bellenger, J.-P., Wichard, T., Xu, Y., & Kraepiel, A. M. L. (2011). Essential metals for
775 nitrogen fixation in a free-living N₂-fixing bacterium: chelation, homeostasis and high
776 use efficiency. *Environmental Microbiology*, *13*(6), 1395–411.

777 <https://doi.org/10.1111/j.1462-2920.2011.02440.x>

778 Bellenger, J.-P., Darnajoux, R., Zhang, X., & Kraepiel, A. M. L. (2020). Biological nitrogen
779 fixation by alternative nitrogenases in terrestrial ecosystems: a review. *Biogeochemistry*,
780 149(1), 53–73. <https://doi.org/10.1007/s10533-020-00666-7>

781 Bertics, V. J., Sohm, J. A., Treude, T., Chow, C. E. T., Capone, D. G., Fuhrman, J. A., &
782 Ziebis, W. (2010). Burrowing deeper into benthic nitrogen cycling: The impact of
783 Bioturbation on nitrogen fixation coupled to sulfate reduction. *Marine Ecology Progress*
784 *Series*, 409, 1–15. <https://doi.org/10.3354/meps08639>

785 Bertics, V. J., Löscher, C. R., Salonen, I., Dale, A. W., Gier, J., Schmitz, R. A., & Treude, T.
786 (2013). Occurrence of benthic microbial nitrogen fixation coupled to sulfate reduction in
787 the seasonally hypoxic Eckernförde Bay, Baltic Sea. *Biogeosciences*, 10(3), 1243–1258.
788 <https://doi.org/10.5194/bg-10-1243-2013>

789 van den Boogaart, K. G., & Tolosana-Delgado, R. (2008). “compositions”: A unified R
790 package to analyze compositional data. *Computers and Geosciences*, 34(4), 320–338.
791 <https://doi.org/10.1016/j.cageo.2006.11.017>

792 Boyd, E. S., Garcia Costas, A. M., Hamilton, T. L., Mus, F., & Peters, J. W. (2015). Evolution
793 of molybdenum nitrogenase during the transition from anaerobic to aerobic metabolism.
794 *Journal of Bacteriology*, 197(9), 1690–1699. <https://doi.org/10.1128/JB.02611-14>

795 Brown, S. M., & Jenkins, B. D. (2014). Profiling gene expression to distinguish the likely
796 active diazotrophs from a sea of genetic potential in marine sediments. *Environmental*
797 *Microbiology*, 16(10), 3128–3142. <https://doi.org/10.1111/1462-2920.12403>

798 Burns, J. A., Zehr, J. P., & Capone, D. G. (2002). Nitrogen-fixing phylotypes of Chesapeake
799 Bay and neuse river estuary sediments. *Microbial Ecology*, 44(4), 336–343.
800 <https://doi.org/10.1007/s00248-002-1000-9>

801 Capone, D. G. (1988). Benthic nitrogen fixation. In T. H. Blackburn & J. Sorensen (Eds.),

802 *Nitrogen cycling in coastal marine environments* (Vol. 139, pp. 498–499). John Wiley &
803 Sons, Ltd. [https://doi.org/10.1016/0769-2609\(88\)90114-7](https://doi.org/10.1016/0769-2609(88)90114-7)

804 Capone, D. G., & Carpenter, E. J. (1982). Nitrogen fixation in the marine environment.
805 *Science*, 217(4565), 1140–1142. <https://doi.org/10.1126/science.217.4565.1140>

806 Caporaso, J. G., Lauber, C. L., Walters, W. A., Berg-Lyons, D., Huntley, J., Fierer, N., et al.
807 (2012). Ultra-high-throughput microbial community analysis on the Illumina HiSeq and
808 MiSeq platforms. *The ISME Journal* 2012 6:8, 6(8), 1621–1624.
809 <https://doi.org/10.1038/ismej.2012.8>

810 Carpenter, E. J., Van Raalte, C. D., & Valiela, I. (1978). Nitrogen fixation by algae in a
811 Massachusetts salt marsh. *Limnology and Oceanography*, 23(2), 318–327.
812 <https://doi.org/10.4319/lo.1978.23.2.0318>

813 Codispoti, L. A. (2007). An oceanic fixed nitrogen sink exceeding 400 Tg N a⁻¹ vs the
814 concept of homeostasis in the fixed-nitrogen inventory. *Biogeosciences*, 4(2), 233–253.
815 <https://doi.org/10.5194/bg-4-233-2007>

816 Davis, L. C., & Wang, Y. L. (1980). In vivo and in vitro kinetics of nitrogenase. *Journal of*
817 *Bacteriology*, 141(3), 1230–1238. <https://doi.org/10.1128/jb.141.3.1230-1238.1980>

818 Dekaezemacker, J., & Bonnet, S. (2011). Sensitivity of N₂ fixation to combined nitrogen
819 forms (NO₃⁻ and NH₄⁺) in two strains of the marine diazotroph *Crocospaera watsonii*
820 (Cyanobacteria). *Marine Ecology Progress Series*, 438, 33–46.
821 <https://doi.org/10.3354/meps09297>

822 Dekas, A. E., Fike, D. A., Chadwick, G. L., Green-Saxena, A., Fortney, J., Connon, S. A., et
823 al. (2018). Widespread nitrogen fixation in sediments from diverse deep-sea sites of
824 elevated carbon loading. *Environmental Microbiology*, 20(12), 4281–4296.
825 <https://doi.org/10.1111/1462-2920.14342>

- 826 Dixon, R., & Kahn, D. (2004). Genetic regulation of biological nitrogen fixation. *Nature*
827 *Reviews. Microbiology*, 2(8), 621–631. <https://doi.org/10.1038/nrmicro954>
- 828 Drozd, J. W., Tubb, R. S., & Postgate, J. R. (1972). A chemostat study of the effect of fixed
829 nitrogen sources on nitrogen fixation, membranes and free amino acids in *Azotobacter*
830 *chroococcum*. *Journal of General Microbiology*, 73(2), 221–232.
831 <https://doi.org/10.1099/00221287-73-2-221>
- 832 Elser, J. J., Bracken, M. E. S., Cleland, E. E., Gruner, D. S., Harpole, W. S., Hillebrand, H.,
833 et al. (2007). Global analysis of nitrogen and phosphorus limitation of primary producers
834 in freshwater, marine and terrestrial ecosystems. *Ecology Letters*, 10(12), 1135–1142.
835 <https://doi.org/10.1111/j.1461-0248.2007.01113.x>
- 836 Foster, S. Q., & Fulweiler, R. W. (2014). Spatial and historic variability of benthic nitrogen
837 cycling in an anthropogenically impacted estuary. *Frontiers in Marine Science*, 1(NOV),
838 56. <https://doi.org/10.3389/fmars.2014.00056>
- 839 Fulweiler, R. W., Nixon, S. W., Buckley, B. A., & Granger, S. L. (2007). Reversal of the net
840 dinitrogen gas flux in coastal marine sediments. *Nature*, 448(7150), 180–182.
841 <https://doi.org/10.1038/nature05963>
- 842 Fulweiler, R. W., Heiss, E. M., Rogener, M. K., Newell, S. E., LeCleir, G. R., Kortebein, S. M.,
843 & Wilhelm, S. W. (2015). Examining the impact of acetylene on N-fixation and the active
844 sediment microbial community. *Frontiers in Microbiology*, 6(MAY).
845 <https://doi.org/10.3389/fmicb.2015.00418>
- 846 Gandy, E. L., & Yoch, D. C. (1988). Relationship between nitrogen-fixing sulfate reducers
847 and fermenters in salt marsh sediments and roots of *Spartina*. *Applied and Environmental*
848 *Microbiology*, 54(8), 2031–2036. <https://doi.org/10.1128/aem.54.8.2031-2036.1988>
- 849 Gier, J., Sommer, S., Löscher, C. R., Dale, A. W., Schmitz, R. A., & Treude, T. (2015).

850 Nitrogen fixation in sediments along a depth transect through the Peruvian oxygen
851 minimum zone. *Biogeosciences Discussions*, 12(17), 14401–14440.
852 <https://doi.org/10.5194/bgd-12-14401-2015>

853 Gier, J., Sommer, S., Löscher, C. R., Dale, A. W., Schmitz, R. A., & Treude, T. (2016).
854 Nitrogen fixation in sediments along a depth transect through the Peruvian oxygen
855 minimum zone. *Biogeosciences*, 13(14), 4065–4080. [https://doi.org/10.5194/bg-13-](https://doi.org/10.5194/bg-13-4065-2016)
856 [4065-2016](https://doi.org/10.5194/bg-13-4065-2016)

857 Glibert, P. M., Wilkerson, F. P., Dugdale, R. C., Raven, J. A., Dupont, C. L., Leavitt, P. R., et
858 al. (2016). Pluses and minuses of ammonium and nitrate uptake and assimilation by
859 phytoplankton and implications for productivity and community composition, with
860 emphasis on nitrogen-enriched conditions. *Limnology and Oceanography*, 61(1), 165–
861 197. <https://doi.org/10.1002/lno.10203>

862 Gloor, G. B., Macklaim, J. M., Pawlowsky-Glahn, V., & Egozcue, J. J. (2017, November 15).
863 Microbiome datasets are compositional: And this is not optional. *Frontiers in*
864 *Microbiology*. Frontiers Media S.A. <https://doi.org/10.3389/fmicb.2017.02224>

865 Gordon, J. K., Shah, V. K., & Brill, W. J. (1981). Feedback inhibition of nitrogenase. *Journal*
866 *of Bacteriology*, 148(3), 884–888. <https://doi.org/10.1128/jb.148.3.884-888.1981>

867 Goto, M., Ando, S., Hachisuka, Y., & Yoneyama, T. (2005). Contamination of diverse *nifH*
868 and *nifH*-like DNA into commercial PCR primers. *FEMS Microbiology Letters*, 246(1),
869 33–38. <https://doi.org/10.1016/j.femsle.2005.03.042>

870 Großkopf, T., & LaRoche, J. (2012). Direct and indirect costs of dinitrogen fixation in
871 *Crocospaera watsonii* WH8501 and possible implications for the nitrogen cycle.
872 *Frontiers in Microbiology*, 3(JUL). <https://doi.org/10.3389/fmicb.2012.00236>

873 Gruber, N., & Galloway, J. N. (2008, January 17). An Earth-system perspective of the global

874 nitrogen cycle. *Nature*. Nature Publishing Group. <https://doi.org/10.1038/nature06592>

875 Hardy, R. W. F., Holsten, R. D., Jackson, E. K., & Burns, R. C. (1968). The acetylene -
876 ethylene assay for N₂ fixation : laboratory and field evaluation. *Plant Physiology*,
877 43(1968), 1185–1207.

878 Hartmann, A., Fu, H., & Burris, R. H. (1986). *Regulation of nitrogenase activity by*
879 *ammonium chloride in Azospirillum spp.* *Journal of Bacteriology*.

880 Heidelberg, J. F., Seshadri, R., Haveman, S. A., Hemme, C. L., Paulsen, I. T., Kolonay, J. F.,
881 et al. (2004). The genome sequence of the anaerobic, sulfate-reducing bacterium
882 *Desulfovibrio vulgaris* Hildenborough. *Nature Biotechnology*, 22(5), 554–559.
883 <https://doi.org/10.1038/nbt959>

884 Heiniger, E. K., & Harwood, C. S. (2015). Posttranslational modification of a vanadium
885 nitrogenase. *MicrobiologyOpen*, 4(4), 597–603. <https://doi.org/10.1002/mbo3.265>

886 Holl, C. M., & Montoya, J. P. (2005). Interactions between nitrate uptake and nitrogen
887 fixation in continuous cultures of the marine diazotroph *Trichodesmium* (Cyanobacteria).
888 *Journal of Phycology*, 41(6), 1178–1183. <https://doi.org/10.1111/j.1529->
889 8817.2005.00146.x

890 Holmes, R. M., Aminot, A., K erouel, R., Hooker, B. A., & Peterson, B. J. (1999). A simple
891 and precise method for measuring ammonium in marine and freshwater ecosystems.
892 *Canadian Journal of Fisheries and Aquatic Sciences*, 56(10), 1801–1808.
893 <https://doi.org/10.1139/f99-128>

894 Hou, L., Wang, R., Yin, G., Liu, M., & Zheng, Y. (2018). Nitrogen fixation in the intertidal
895 sediments of the Yangtze estuary: Occurrence and environmental implications. *Journal*
896 *of Geophysical Research: Biogeosciences*, 123(3), 936–944.
897 <https://doi.org/10.1002/2018JG004418>

898 Huergo, L. F., & Dixon, R. (2015). The emergence of 2-oxoglutarate as a master regulator
899 metabolite. *Microbiology and Molecular Biology Reviews*, 79(4), 419–435.
900 <https://doi.org/10.1128/membr.00038-15>

901 Inomura, K., Bragg, J., & Follows, M. J. (2017). A quantitative analysis of the direct and
902 indirect costs of nitrogen fixation: A model based on *Azotobacter vinelandii*. *ISME*
903 *Journal*, 11(1), 166–175. <https://doi.org/10.1038/ismej.2016.97>

904 Javelle, A., Severi, E., Thornton, J., & Merrick, M. (2004). Ammonium sensing in *Escherichia*
905 *coli*: Role of the ammonium transporter AmtB and AmtB-GlnK complex formation.
906 *Journal of Biological Chemistry*, 279(10), 8530–8538.
907 <https://doi.org/10.1074/jbc.M312399200>

908 Jayakumar, A., Chang, B. X., Widner, B., Bernhardt, P., Mulholland, M. R., & Ward, B. B.
909 (2017). Biological nitrogen fixation in the oxygen-minimum region of the eastern tropical
910 North Pacific ocean. *ISME Journal*, 11(10), 2356–2367.
911 <https://doi.org/10.1038/ismej.2017.97>

912 Kapili, B. J., Barnett, S. E., Buckley, D. H., & Dekas, A. E. (2020). Evidence for
913 phylogenetically and catabolically diverse active diazotrophs in deep-sea sediment.
914 *ISME Journal*, 14(4), 971–983. <https://doi.org/10.1038/s41396-019-0584-8>

915 Kessler, P. S., Daniel, C., & Leigh, J. A. (2001). Ammonia switch-off of nitrogen fixation in
916 the methanogenic archaeon *Methanococcus maripaludis*: Mechanistic features and
917 requirement for the novel GlnB homologues, Nif1 and Nif2. *Journal of Bacteriology*,
918 183(3), 882–889. <https://doi.org/10.1128/JB.183.3.882-889.2001>

919 Kleiner, D. (1974). Quantitative relations for the repression of nitrogenase synthesis in
920 *Azotobacter vinelandii* by ammonia. *Archives of Microbiology*, 101(1), 153–159.
921 <https://doi.org/10.1007/BF00455935>

- 922 Kleiner, D. (1985). Bacterial ammonium transport. *FEMS Microbiology Letters*, 32(2), 87–
923 100. [https://doi.org/10.1016/0378-1097\(85\)90059-X](https://doi.org/10.1016/0378-1097(85)90059-X)
- 924 Knapp, A. N. (2012). The sensitivity of marine N₂ fixation to dissolved inorganic nitrogen.
925 *Frontiers in Microbiology*, 3(OCT), 374. <https://doi.org/10.3389/fmicb.2012.00374>
- 926 Kuzyakov, Y., & Xu, X. (2013). Competition between roots and microorganisms for nitrogen:
927 Mechanisms and ecological relevance. *New Phytologist*, 198(3), 656–669.
928 <https://doi.org/10.1111/nph.12235>
- 929 Lespinat, P. A., Berlier, Y. M., Fauque, G. D., Toci, R., Denariáz, G., & LeGall, J. (1987). The
930 relationship between hydrogen metabolism, sulfate reduction and nitrogen fixation in
931 sulfate reducers. *Journal of Industrial Microbiology*, 1(6), 383–388.
932 <https://doi.org/10.1007/BF01569336>
- 933 Masepohl, B., Drepper, T., Paschen, A., Gross, S., Pawlowski, A., Raabe, K., et al. (2002).
934 Regulation of nitrogen fixation in the phototrophic purple bacterium *Rhodobacter*
935 *capsulatus*. *Journal of Molecular Microbiology and Biotechnology*, 4(3), 243–8.
- 936 McMurdie, P. J., & Holmes, S. (2013). Phyloseq: An R package for reproducible interactive
937 analysis and graphics of microbiome census data. *PLoS ONE*, 8(4).
938 <https://doi.org/10.1371/journal.pone.0061217>
- 939 McRose, D. L., Zhang, X., Kraepiel, A. M. L., & Morel, F. M. M. (2017). Diversity and activity
940 of alternative nitrogenases in sequenced genomes and coastal environments. *Frontiers*
941 *in Microbiology*, 8, 267. <https://doi.org/10.3389/fmicb.2017.00267>
- 942 Metzger, E., Barbe, A., Cesbron, F., Thibault de Chanvalon, A., Jauffrais, T., Jézéquel, D., &
943 Mouret, A. (2019). Two-dimensional ammonium distribution in sediment pore waters
944 using a new colorimetric diffusive equilibration in thin-film technique. *Water Research X*,
945 2, 100023. <https://doi.org/10.1016/j.wroa.2018.100023>

946 Mohr, W., Großkopf, T., Wallace, D. W. R., & LaRoche, J. (2010). Methodological
947 underestimation of oceanic nitrogen fixation rates. *PLoS ONE*, 5(9), 1–7.
948 <https://doi.org/10.1371/journal.pone.0012583>

949 Montoya, J. P., Voss, M., Kähler, P., & Capone, D. G. (1996). A simple , high-precision ,
950 high-sensitivity tracer assay for N₂ fixation. *Applied and Environmental Microbiology*,
951 62(3), 986–993.

952 Mulholland, M. R., Ohki, K., & Capone, D. G. (2001). Nutrient controls on nitrogen uptake
953 and metabolism by natural populations and cultures of *Trichodesmium* (Cyanobacteria).
954 *Journal of Phycology*, 37(6), 1001–1009. [https://doi.org/10.1046/j.1529-](https://doi.org/10.1046/j.1529-8817.2001.00080.x)
955 [8817.2001.00080.x](https://doi.org/10.1046/j.1529-8817.2001.00080.x)

956 Newell, S. E., Pritchard, K. R., Foster, S. Q., & Fulweiler, R. W. (2016). Molecular evidence
957 for sediment nitrogen fixation in a temperate New England estuary. *PeerJ*, 2016(1),
958 e1615. <https://doi.org/10.7717/peerj.1615>

959 Newell, S. E., McCarthy, M. J., Gardner, W. S., & Fulweiler, R. W. (2016). Sediment nitrogen
960 fixation: a call for re-evaluating coastal N budgets. *Estuaries and Coasts*, 39(6), 1626–
961 1638. <https://doi.org/10.1007/s12237-016-0116-y>

962 Ohki, K., Zehr, J. P., Falkowski, P. G., & Fujita, Y. (1991). Regulation of nitrogen-fixation by
963 different nitrogen sources in the marine non-heterocystous cyanobacterium
964 *Trichodesmium* sp. NIBB1067. *Archives of Microbiology*, 156(5), 335–337.
965 <https://doi.org/10.1007/BF00248706>

966 Oksanen, J. F., Blanchet, G., Friendly, M., Kindt, R., Legendre, P., & McGlenn, D. (2019).
967 vegan: Community Ecology Package.

968 Patriquin, D. G., & Keddy, C. (1978). Nitrogenase activity (acetylene reduction) in a Nova
969 Scotian salt marsh: Its association with angiosperms and the influence of some edaphic

970 factors. *Aquatic Botany*, 4(C), 227–244. [https://doi.org/10.1016/0304-3770\(78\)90021-9](https://doi.org/10.1016/0304-3770(78)90021-9)

971 Payne, W. J., & Grant, M. A. (1982). Influence of acetylene on growth of sulfate-respiring
972 bacteria. *Applied and Environmental Microbiology*, 43(3), 727–30.
973 <https://doi.org/10.1128/AEM.43.3.727-730.1982>

974 Postgate, J. R., & Kent, H. M. (1984). Derepression of nitrogen fixation in *Desulfovibrio gigas*
975 and its stability to ammonia or oxygen stress in vivo. *Journal of general microbiology*
976 (Vol. 130).

977 Price, M. N., Dehal, P. S., & Arkin, A. P. (2010). FastTree 2 - Approximately maximum-
978 likelihood trees for large alignments. *PLoS ONE*, 5(3), e9490.
979 <https://doi.org/10.1371/journal.pone.0009490>

980 Riederer-Henderson, M. A., & Wilson, P. W. (1970). Nitrogen fixation by sulphate-reducing
981 bacteria. *Journal of General Microbiology*, 61(1), 27–31.
982 <https://doi.org/10.1099/00221287-61-1-27>

983 Schreiber, F., Littmann, S., Lavik, G., Escrig, S., Meibom, A., Kuypers, M. M. M., &
984 Ackermann, M. (2016). Phenotypic heterogeneity driven by nutrient limitation promotes
985 growth in fluctuating environments. *Nature Microbiology*, 1(6), 1–7.
986 <https://doi.org/10.1038/nmicrobiol.2016.55>

987 Sim, M. S., Wang, D. T., Zane, G. M., Wall, J. D., Bosak, T., & Ono, S. (2013). Fractionation
988 of sulfur isotopes by *Desulfovibrio vulgaris* mutants lacking hydrogenases or type I
989 tetraheme cytochrome c3. *Frontiers in Microbiology*, 4(JUN).
990 <https://doi.org/10.3389/fmicb.2013.00171>

991 Sohm, J. A., Webb, E. A., & Capone, D. G. (2011). Emerging patterns of marine nitrogen
992 fixation. *Nature Reviews Microbiology*, 9(7), 499–508.
993 <https://doi.org/10.1038/nrmicro2594>

- 994 Steppe, T. F., & Paerl, H. W. (2005). Nitrogenase activity and nifH expression in a marine
995 intertidal microbial mat. *Microbial Ecology*, 49(2), 315–324.
996 <https://doi.org/10.1007/s00248-004-0245-x>
- 997 Sweet, W. J., & Burris, R. H. (1981). Inhibition of nitrogenase activity by NH₄⁺ in
998 *Rhodospirillum rubrum*. *Journal of Bacteriology*, 145(2), 824–831.
999 <https://doi.org/10.1128/jb.145.2.824-831.1981>
- 1000 Tichi, M. A., & Tabita, F. R. (2000). Maintenance and control of redox poise in *Rhodobacter*
1001 *capsulatus* strains deficient in the Calvin-Benson-Bassham pathway. *Archives of*
1002 *Microbiology*, 174(5), 322–333. <https://doi.org/10.1007/s002030000209>
- 1003 Tubb, R. S., & Postgate, J. R. (1973). Control of nitrogenase synthesis in *Klebsiella*
1004 *pneumoniae*. *Journal of General Microbiology*, 79(1), 103–117.
1005 <https://doi.org/10.1099/00221287-79-1-103>
- 1006 Voss, M., Bange, H. W., Dippner, J. W., Middelburg, J. J., Montoya, J. P., & Ward, B. (2013).
1007 The marine nitrogen cycle: Recent discoveries, uncertainties and the potential relevance
1008 of climate change. *Philosophical Transactions of the Royal Society B: Biological*
1009 *Sciences*, 368(1621). <https://doi.org/10.1098/rstb.2013.0121>
- 1010 Welsh, D. T., Bourgués, S., De Wit, R., & Herbert, R. A. (1996). Seasonal variations in
1011 nitrogen-fixation (acetylene reduction) and sulphate-reduction rates in the rhizosphere
1012 of *Zostera noltii*: Nitrogen fixation by sulphate-reducing bacteria. *Marine Biology*, 125(4),
1013 619–628. <https://doi.org/10.1007/BF00349243>
- 1014 Welsh, David T. (2000, January 1). Nitrogen fixation in seagrass meadows: Regulation,
1015 plant-bacteria interactions and significance to primary productivity. *Ecology Letters*.
1016 John Wiley & Sons, Ltd. <https://doi.org/10.1046/j.1461-0248.2000.00111.x>
- 1017 Westlake, D. W., & Wilson, P. W. (1959). Molecular hydrogen and nitrogen fixation by

- 1018 Clostridium pasteurianum. *Canadian Journal of Microbiology*, 5, 617–620.
1019 <https://doi.org/10.1139/m59-075>
- 1020 Winogradsky, M. S. (1895). Sur l'assimilation de l'azote libre de l'atmosphère par les
1021 microbes. *Arch. Sci. Biol. St. Petersb.*, (3), 297–352.
- 1022 Yoch, D. C., & Whiting, G. J. (1986). Evidence for NH₄⁺ switch-off regulation of nitrogenase
1023 activity by bacteria in salt marsh sediments and roots of the grass *Spartina alterniflora*.
1024 *Applied and Environmental Microbiology*, 51(1), 143–149.
1025 <https://doi.org/10.1128/aem.51.1.143-149.1986>
- 1026 Zehr, J. P., & Kudela, R. M. (2011). Nitrogen cycle of the open ocean: From genes to
1027 ecosystems. *Annual Review of Marine Science*, 3, 197–225.
1028 <https://doi.org/10.1146/annurev-marine-120709-142819>
- 1029 Zehr, J. P., & McReynolds, L. A. (1989). Use of degenerate oligonucleotides for amplification
1030 of the nifH gene from the marine cyanobacterium *Trichodesmium thiebautii*. *Applied*
1031 *and Environmental Microbiology*, 55(10), 2522–2526.
1032 <https://doi.org/10.1128/aem.55.10.2522-2526.1989>
- 1033 Zehr, J. P., Mellon, M. T., & Zani, S. (1998). New nitrogen-fixing microorganisms detected in
1034 oligotrophic oceans by amplification of nitrogenase (nifH) genes. *Applied and*
1035 *Environmental Microbiology*, 64(9), 3444–3450. [https://doi.org/10.1128/aem.64.9.3444-](https://doi.org/10.1128/aem.64.9.3444-3450.1998)
1036 [3450.1998](https://doi.org/10.1128/aem.64.9.3444-3450.1998)
- 1037 Zehr, J. P., Jenkins, B. D., Short, S. M., & Steward, G. F. (2003). Nitrogenase gene diversity
1038 and microbial community structure: A cross-system comparison. *Environmental*
1039 *Microbiology*, 5(7), 539–554. <https://doi.org/10.1046/j.1462-2920.2003.00451.x>
- 1040 Zhang, X., McRose, D. L., Darnajoux, R., Bellenger, J.-P., Morel, F. M. M., & Kraepiel, A.
1041 M. L. L. (2016). Alternative nitrogenase activity in the environment and nitrogen cycle

1042 implications. *Biogeochemistry*, 127(2–3), 189–198. <https://doi.org/10.1007/s10533-016->
1043 0188-6

1044 Zhang, X., Ward, B. B., & Sigman, D. M. (2020, June 24). Global nitrogen cycle: critical
1045 enzymes, organisms, and processes for nitrogen budgets and dynamics. *Chemical*
1046 *Reviews*. American Chemical Society. <https://doi.org/10.1021/acs.chemrev.9b00613>

1047 Zheng, L., Kostrewa, D., Bernèche, S., Winkler, F. K., & Li, X. D. (2004). The mechanism of
1048 ammonia transport based on the crystal structure of AmtB of *Escherichia coli*.
1049 *Proceedings of the National Academy of Sciences of the United States of America*,
1050 101(49), 17090–17095. <https://doi.org/10.1073/pnas.0406475101>

1051

1052 **Figure Caption:**

1053 **Figure 1: Effect of ammonium on growth and biological nitrogen fixation (BNF) in**
1054 ***Desulfovibrio vulgaris* var. Hildenborough (DvH, Panels A, C and D) and *Clostridium***
1055 ***pasteurianum* (Cp, Panel B).** (A) Representative growth curves of *DvH* for initial $[\text{NH}_4^+]$ at
1056 the background concentration in diazotrophic media ($< 10 \mu\text{M}$), $500 \mu\text{M}$, and $3,000 \mu\text{M}$.
1057 Growth was supported by 30 mM pyruvate and sulfate. Error bars are standard deviations
1058 from one experiment ($n=3$). Growth rates are calculated from independent replicates ($n=3$)
1059 (B) Representative growth curves of *Cp* for initial $[\text{NH}_4^+]$ at the background concentration in
1060 diazotrophic media ($< 10 \mu\text{M}$), $500 \mu\text{M}$, and $3,000 \mu\text{M}$. Growth was supported by
1061 fermentation of sucrose. Error bars are standard deviations from one experiment ($n=3$).
1062 Growth rates are calculated from independent replicates ($n=3$)(C) Relative BNF activity of
1063 *DvH* was measured as the Acetylene Reduction Rate at 3h, 6h and 26h after addition of
1064 NH_4^+ (to concentrations of 10, 30, 100, 300, and $3,000 \mu\text{M}$) compared to BNF activity before
1065 addition to *DvH* grown under N_2 -fixing conditions. Symbols represent individual samples

1066 from a single experiment. (D) Estimated contribution of BNF to total N supply after
1067 ammonium additions. Error bars represent standard errors of the mean.

1068 **Figure 2: Effect of ammonium concentration on biological nitrogen fixation (BNF)**
1069 **activity in incubations of sulfate-reducing and fermenting microbes in culture and in**
1070 **sediments.** (A-C) Medium $[\text{NH}_4^+]$ (blue circles) and BNF activity (as accumulation of
1071 headspace ethylene, green squares for NH_4^+ -amended) before and after addition of NH_4^+ to
1072 nitrogen limited, diazotrophic cultures of *Desulfovibrio vulgaris* var. Hildenborough (*DvH*) (A),
1073 *Clostridium pasteurianum* (*Cp*) (B), and Barnegat Bay salt marsh enrichment strain SRBB2
1074 (C) at OD ~ 0.1 (Supplementary Figs. S3-S5). Open symbols show BNF as ethylene
1075 (square) and dissolved $[\text{NH}_4^+]$ (circle) in control experiments without addition of NH_4^+ . (C-E)
1076 Dissolved $[\text{NH}_4^+]$ (blue circles) and N_2 fixed equivalent (green squares, headspace ethylene
1077 for ARA and ^{15}N enrichment of particulate organic matter for ^{15}N tracer) over time in salt
1078 marsh sediment slurry incubations using ARA (C-D) and ^{15}N tracer methods (E). Additions
1079 are indicated with arrows. Only one representative replicate is shown to illustrate results for
1080 reasons of clarity. All incubation data (*Desulfovibrio vulgaris* n=6, SRBB1 n=2, SRBB2 n=2,
1081 salt marsh slurry n=10 for each method) are found in Supplementary Figures S3-S6 and
1082 summarized in Figure 3. Dashed lines illustrate interpolation of the BNF rate before and after
1083 NH_4^+ addition to estimate T_R , the time from ammonium addition to BNF inhibition.

1084 **Figure 2: Effect of ammonium concentration on biological nitrogen fixation (BNF)**
1085 **activity in incubations of sulfate-reducing microbes in culture and in sediments.** (A
1086 and B) Medium $[\text{NH}_4^+]$ (blue circles) and BNF activity (as accumulation of headspace
1087 ethylene, green squares for NH_4^+ -amended) before and after addition of NH_4^+ to nitrogen
1088 limited, diazotrophic cultures of *Desulfovibrio vulgaris* var. Hildenborough (*DvH*) (A) and
1089 Barnegat Bay salt marsh enrichment strain SRBB2 at $\text{OD}_{600} \sim 0.1$ (Supplementary Fig. S3
1090 and S4). Open square symbols show control experiments without addition of ammonium. (C
1091 and D) Dissolved $[\text{NH}_4^+]$ (blue circles) and N_2 fixed equivalent (green squares, headspace
1092 ethylene for ARA and ^{15}N enrichment of particulate organic matter for ^{15}N tracer) over time in

1093 salt marsh sediment slurry incubations using ARA (C) and ^{15}N tracer methods (D). Additions
1094 are indicated with arrows. Only one representative replicate is shown to illustrate results for
1095 reasons of clarity. All incubation data (*Desulfovibrio vulgaris* n=6, SRBB1 n=2, SRBB2 n=2,
1096 salt marsh slurry n=10 for each method) are found in Supplementary Figures S3-S6 and
1097 summarized in Figure 3. Dashed lines illustrate interpolation of the BNF rate before and after
1098 NH_4^+ addition to estimate T_R , the time from ammonium addition to BNF inhibition.

1099 **Figure 3: Determination of threshold ammonium concentration (95th percentile) for**
1100 **inhibition of biological nitrogen fixation (BNF) in liquid cultures and sediment slurries.**
1101 Combined results from incubations of *Desulfovibrio vulgaris* var. Hildenborough and
1102 SRBB1&2 consortia enriched from NJ salt marshes (A), ARA (B), and ^{15}N tracer (C) slurry
1103 incubations. BNF rates are the slope between time points from Figure 2. Blue boxes indicate
1104 the range of ammonium concentrations at which BNF was detected; black lines indicate
1105 average ammonium concentration, and dotted lines the 95-percentile (*i.e.* threshold values).
1106 The symbols distinguish data for BNF onset before (closed symbols) and BNF resumption
1107 after (open symbols) NH_4^+ addition. Panel C shows no post-addition data as BNF activity
1108 never resumed in ^{15}N tracer incubations of sediment (See Supplementary Fig. S6 and Fig.
1109 2D). In panel B, post addition data for the 4 of 10 ARA incubations showing abnormal OPA
1110 measurements (See Supplementary Discussion) were highlighted with red stars.

1111 **Figure 4: Microbial composition of diazotroph community in salt marsh sediment**
1112 **incubations.** (A) Phylogeny of the top 500 *nifH* genes OTUs (n=497) and the most
1113 abundant *nifH* transcripts OTUs (n=55, relative abundance>0.2%, total count >1000) from salt
1114 marsh slurry incubations relative to a representative subset (n=152) of a recently curated
1115 *nifH* library (Kapilli et al. 2020). Information on *nifH* genes for *Desulfovibrio vulgaris* v.
1116 Hildenborough (*DvH*), and SRBB1 and SRBB2 enrichments consortia (n=46) are also shown.
1117 (B) Heatmap of *nifH* genes OTU relative abundance (log-scale) at the end of incubation with
1118 class-level information for the 500 first OTUs (bottom bar plot, > 80 % total abundance) and
1119 detailed phylogeny and closest relatives for the most abundant sequences (left panel, OTUs

1120 with relative abundance >0.2% & total count >1000, n=59). Hierarchical clustering of
1121 individual sediment samples based on *nifH* composition (top left of panel) shows the
1122 relationship between sample *nifH* genes composition, incubation condition (ARA vs. ¹⁵N),
1123 and geographical origin of the sediments. Purple box highlights low DNA samples with *nifH*
1124 composition similar to that of control extraction samples (reagent blank). Initial condition
1125 represents the samples before incubation.

1126

1127 **Figure 5: Relationships between nitrogenase activity, microbial diversity, and**
1128 **sediment biogeochemical characteristics in sediment incubation.** (A) Changes in
1129 richness (number of unique OTUs) in nitrogen fixer *nifH* transcripts at the end of incubation
1130 as a function of final ammonium concentrations (n=10). Symbol shade is proportional to the
1131 final BNF activity. (B) Discrimination analysis of nitrogen fixer communities (CAP analysis on
1132 Bray-Curtis distance). (C) Discriminant analysis of sediment biogeochemical activity and
1133 characteristics (redundancy analysis). In B and C, samples using acetylene reduction assay
1134 and ¹⁵N tracer are highlighted in blue and green, respectively (shaded ovals represent 95%
1135 confidence ellipses) and axes show the percent of variance explained and the statistical
1136 significance for each explanatory axis as estimated using permutation Anova. Variables Bold
1137 are statistically significant in the model. In panel B, results were unchanged when we control
1138 for the origin of the sediment (NJ, NH, and MA).

1139 **Figure 6: Theoretical model for ammonium threshold for biological nitrogen fixation in**
1140 **benthic environments.** (A) Overview of the Michaelis-Menten framework for NH_4^+
1141 sensitivity applied to N-fixers in benthic environment, showing the effect of increasing pore
1142 water ammonium with depth on the transition from diazotrophy to ammoniotrophy. (B)
1143 Compilation of experimental data of model sulfate reducers *D. vulgaris* H. (ARA, N = 6 + 3
1144 controls), SRBB enrichments (ARA, N = 4 + 2 controls), and three salt marshes of the
1145 Northeastern US (both ARA and ¹⁵N, N=20) for $[\text{NH}_4^+] < 100 \mu\text{M}$. The red dashed vertical

1146 line shows the 95-percentile $[\text{NH}_4^+]$ (*i.e.* threshold value), and the dashed horizontal line
1147 indicated where BNF is 95% inhibited by ambient ammonium. (C) Frequency distribution of
1148 threshold depth (*i.e.*, depth at which $[\text{NH}_4^+]_{\text{threshold}}$ was reached) derived from literature review
1149 of 26 study in several benthic environments (151 sites, 334 replicates, Supplementary Fig.
1150 S12 and Table S1). The red line represents cumulative frequencies, and the dashed vertical
1151 line represent the median value. (D) Geographic location and threshold depth (color scale) of
1152 reviewed study sites separate by benthic area (shape). Replicate numbers are proportional
1153 to point size.

Figure 1.

Figure 2.

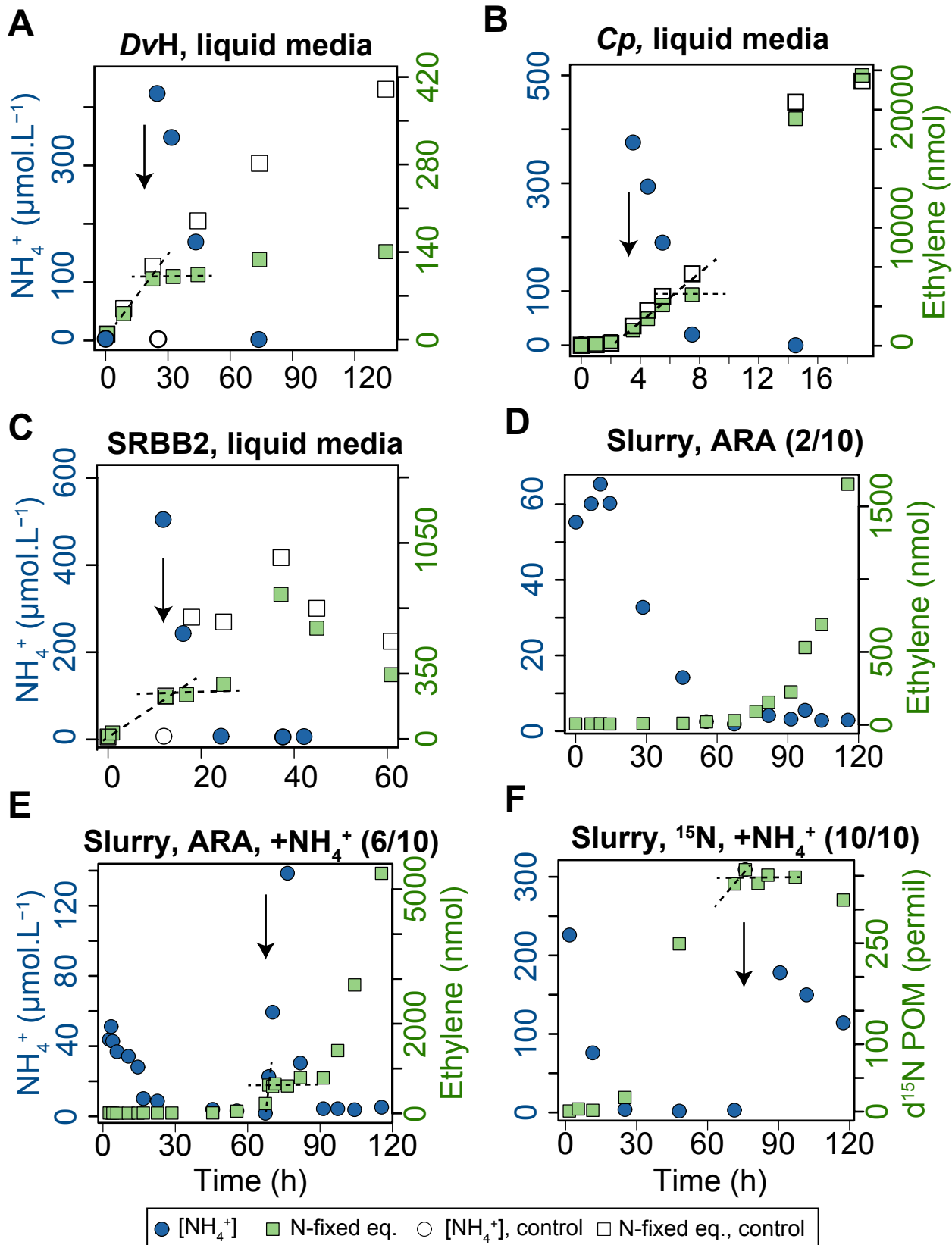


Figure 3.

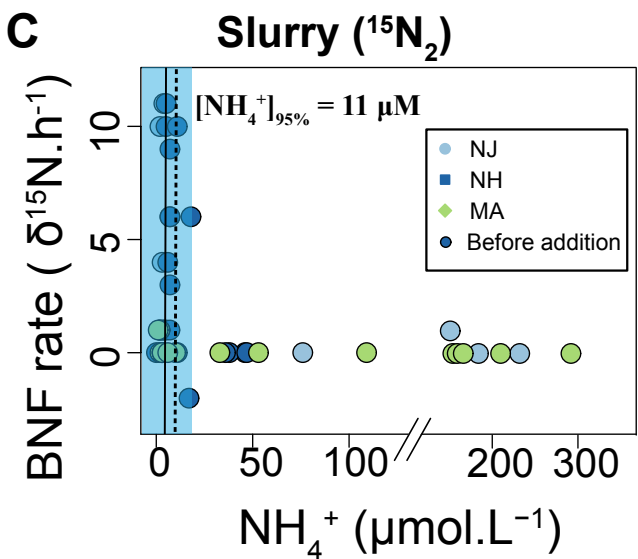
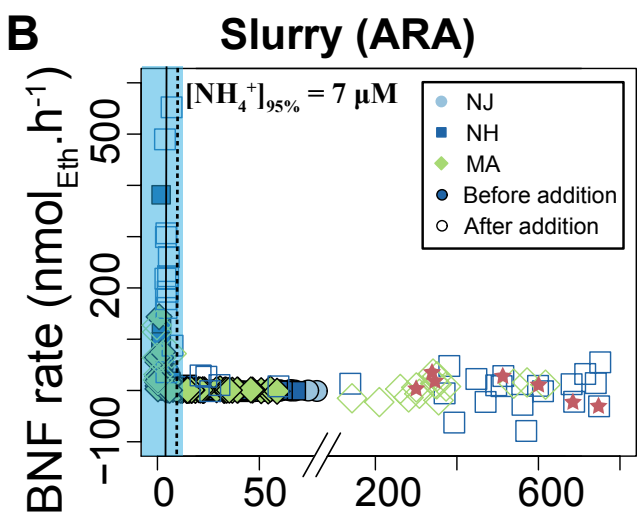
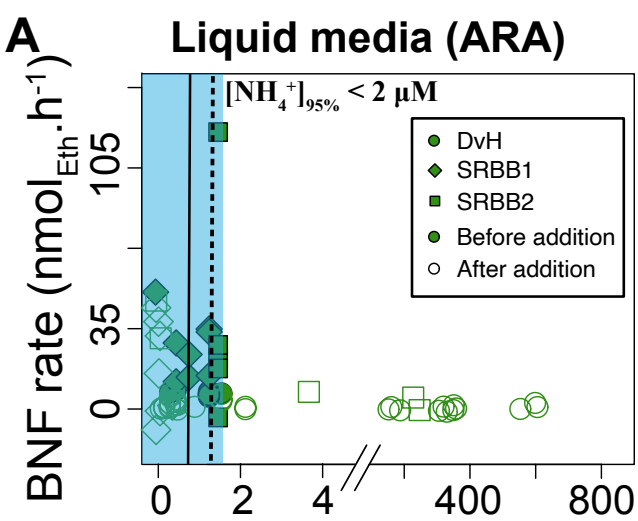


Figure 4.

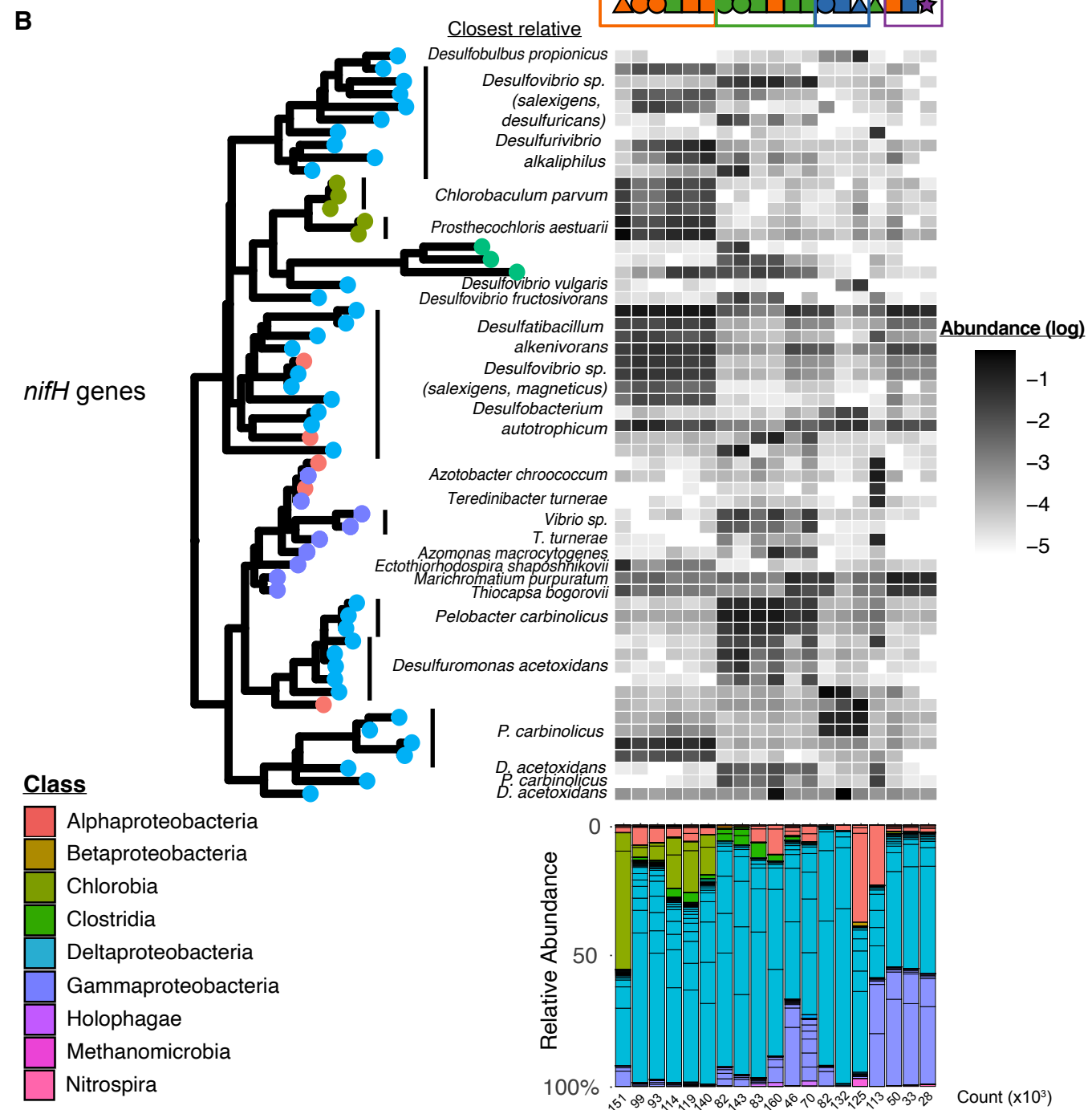
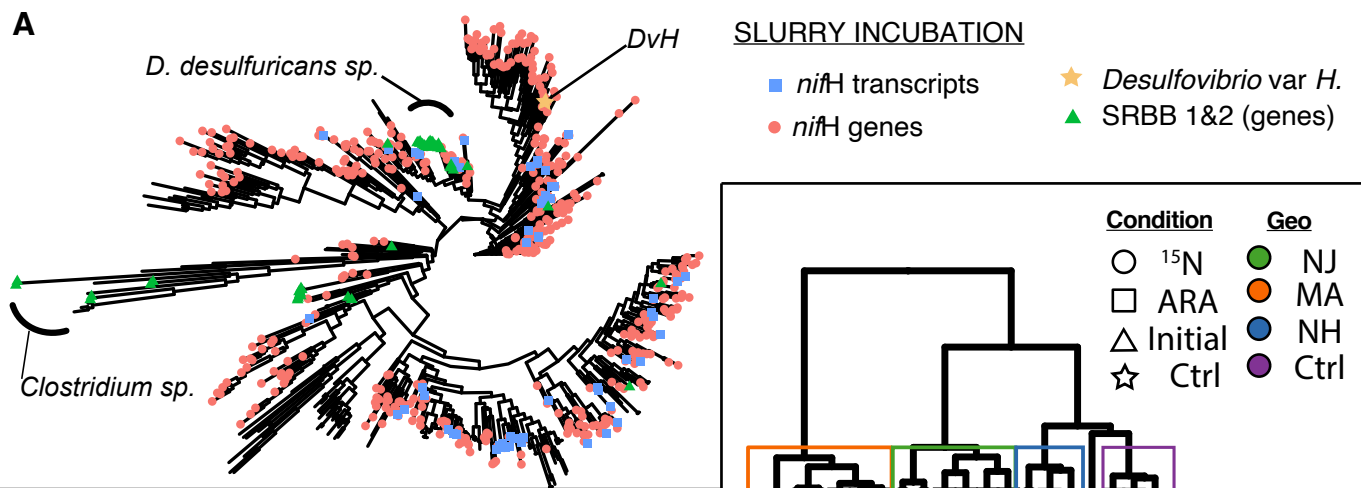


Figure 5.

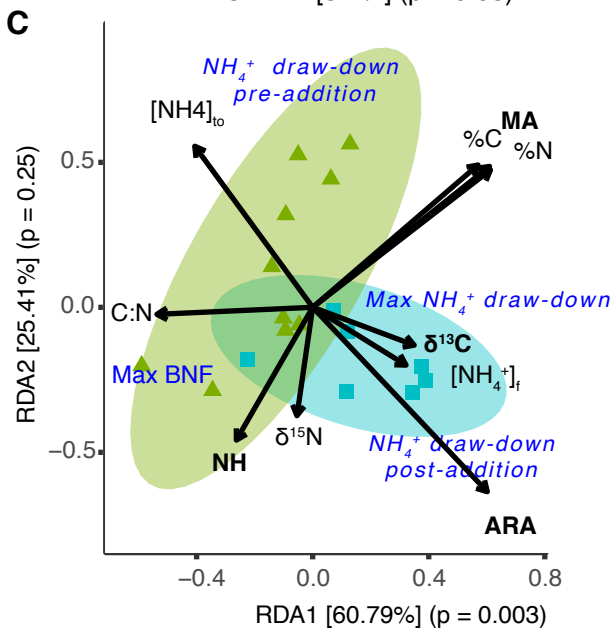
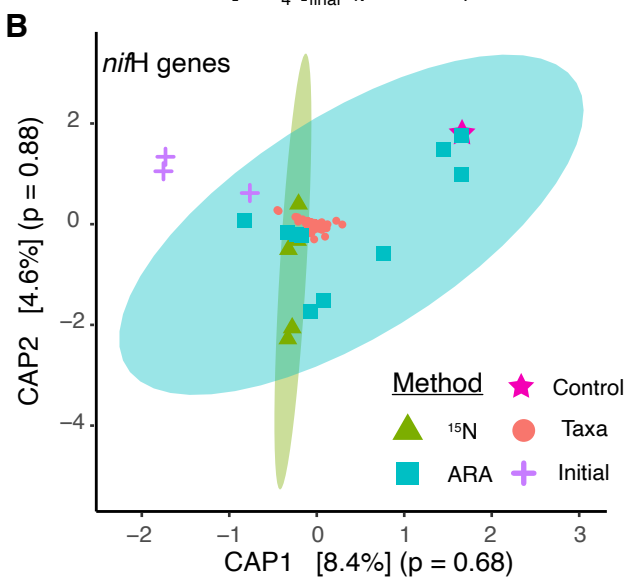
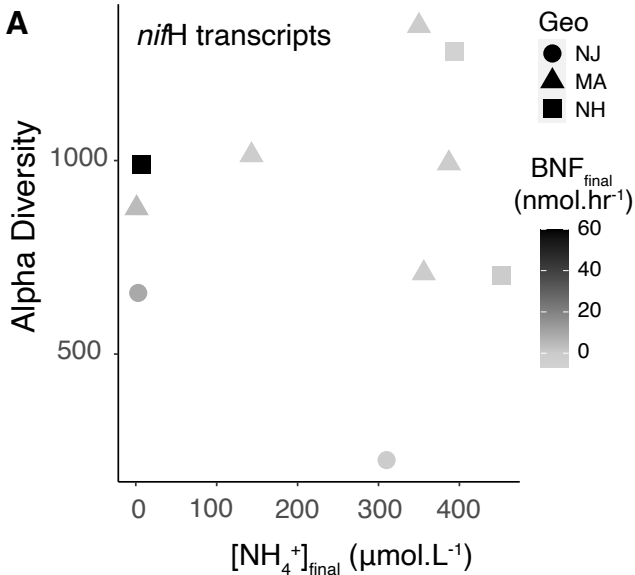


Figure 6.

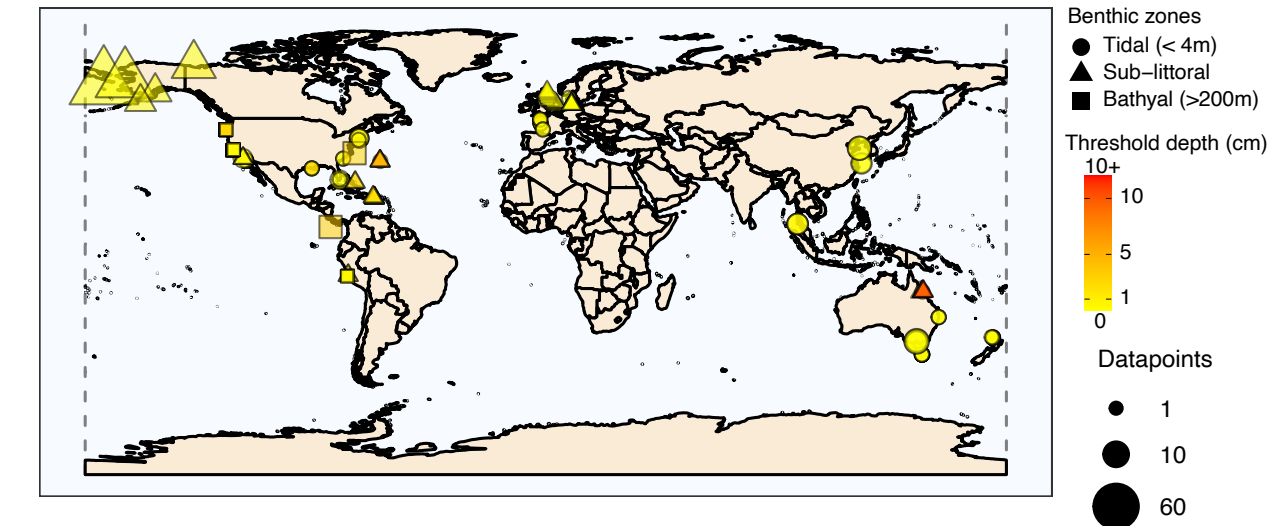
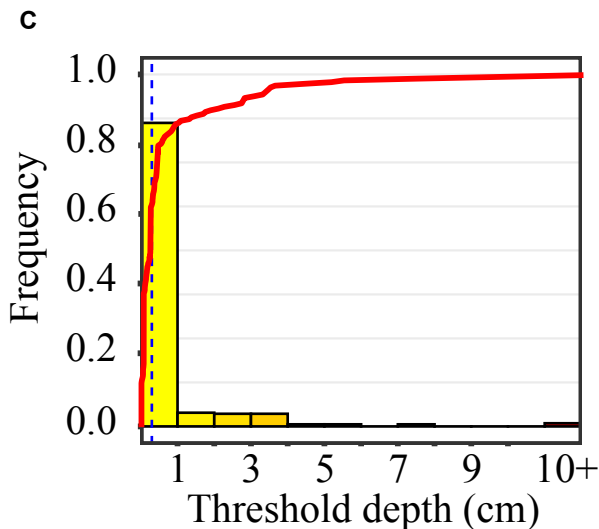
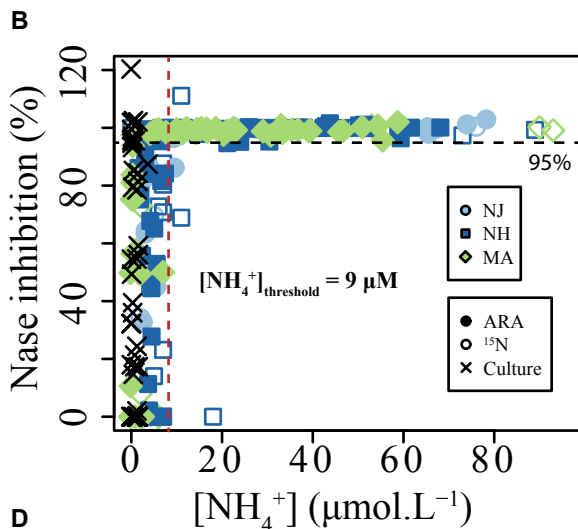
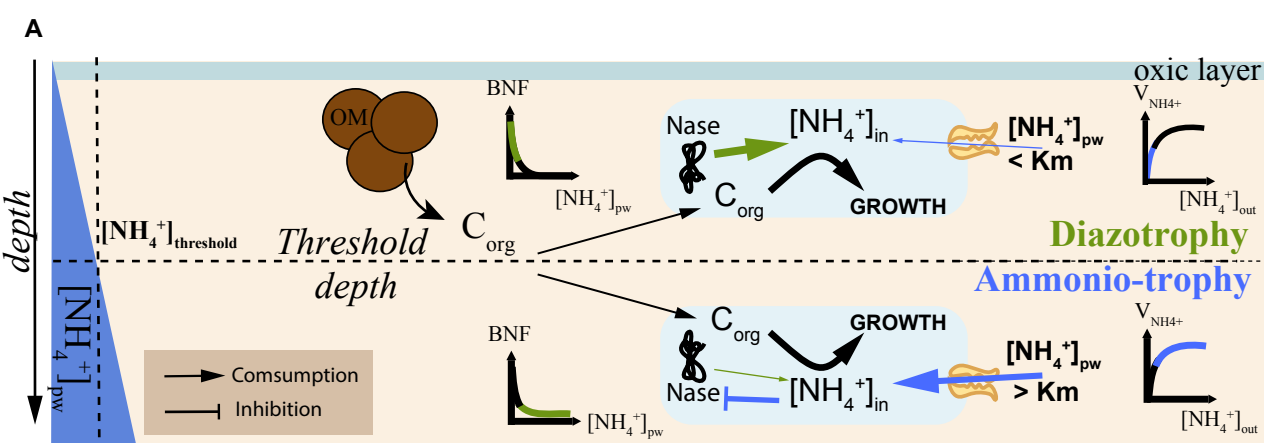


Table 1 : Sediments carbon and nitrogen compositions

| | %C¹ | SD*_{intra} (n=10) | %N | SD_{intra} (n=10) | C:N² | SD_{intra} (n=10) | δ¹³C | SD_{intra} (n=10) | δ¹⁵N | SD_{intra} (n=10) |
|--------------------------------|-----------------------|--------------------------------------|-------------|-------------------------------------|------------------------|-------------------------------------|------------------------|-------------------------------------|------------------------|-------------------------------------|
| Barnaget Bay (NJ) | 6.7 | 3.4 | 0.30 | 0.18 | 28.3 | 7.0 | -27.7 | 0.4 | 2.2 | 0.9 |
| <i>SEM** (n=2)</i> | <i>0.3</i> | <i>0.1</i> | <i>0.01</i> | <i>0.01</i> | <i>0.4</i> | <i>2.6</i> | <i>0.2</i> | <i>0.1</i> | <i>0.2</i> | <i>0.6</i> |
| Great Bay (NH) | 5.4 | 0.9 | 0.43 | 0.07 | 14.7 | 0.5 | -15.5 | 0.2 | 5.1 | 0.4 |
| <i>SEM (n=4)</i> | <i>0.2</i> | <i>0.1</i> | <i>0.01</i> | <i>0.01</i> | <i>0.1</i> | <i>0.1</i> | <i>0.1</i> | <i>0.1</i> | <i>0.1</i> | <i>0.2</i> |
| Sippewissett Marsh (MA) | 22.2 | 6.9 | 1.74 | 0.53 | 14.9 | 0.3 | -18.1 | 0.4 | 3.2 | 0.4 |
| <i>SEM (n=4)</i> | <i>1.1</i> | <i>0.5</i> | <i>0.08</i> | <i>0.05</i> | <i>0.2</i> | <i>0.0</i> | <i>0.1</i> | <i>0.2</i> | <i>0.1</i> | <i>0.1</i> |

¹. %C and %N are on a mass basis relative to oven-dried sediments ($g_{\text{element}} \cdot g_{\text{ODW}}^{-1}$). ². C:N are molar ratio.

*SD_{intra} represents sample heterogeneity, as the SD of 10 replicates taken from the same sample over multiple timepoints and averaged per sediment geography.

**SEM represents the standard error of the mean for each sediment geography.